Research Square

Preprints are preliminary reports that have not undergone peer review.
They should not be considered conclusive, used to inform clinical practice,
or referenced by the media as validated information.

Transcriptomic and Systematic Analyses Reveal *TabZIP* Family Members Involved in the Response to Different Concentrations of Auxin in Wheat Root

Tian Xinyu
Northwest A&F University: College of Agronomy, State Key Laboratory of Crop Stress Biology for Arid Areas
Fang Yan
Northwest A&F University:State Key Laboratory of Soil Erosion and Dryland Farming on the Loess Plateau
Jia Ziyao
Northwest A&F University:College of Agronomy, State Key Laboratory of Crop Stress Biology for Arid Areas
Wang Zhonghua
Northwest A&F University: College of Agronomy, State Key Laboratory of Crop Stress Biology for Arid Areas
Wang Jun (bbrwangjun@nwafu.edu.cn)
Northwest A&F University: Northwest Agriculture and Forestry University https://orcid.org/0000-0002-9229-8742

Research article

Keywords: Auxin Response, TabZIP, Transcriptomic Analysis, Wheat (Triticum aestivum)

Posted Date: December 1st, 2020

DOI: https://doi.org/10.21203/rs.3.rs-114349/v1

License: This work is licensed under a Creative Commons Attribution 4.0 International License. Read Full License

Abstract

Background

Auxin involved in many aspects of root development and physiology which is considered a potential target for improving crop quality and yield. Yet, there has been no systematic investigation on roots underlying the response to different concentrations of auxin. This study evaluated the effects of different concentrations of auxin on the wheat root transcriptome. We also investigated the wheat *bZIP* transcription factor family and preliminarily analyzed the structural function of the members responding to different concentrations of auxin.

Results

In response to 1 μM auxin, 308 and 326 genes whose expression were upregulated and downregulated, respectively, were identified in wheat roots. However, there were 6118 and 2333 genes whose expression were downregulated and upregulated, respectively, in response to 50 μM auxin. GO enrichment and KEGG pathway analyses revealed that the inhibitory effect of 1 μM auxin in roots manifested as an enrichment of the glycolysis/gluconeogenesis and glutathione metabolism pathways. Enrichment of the phenylpropanoid biosynthesis and plant-pathogen interaction pathways in response to 50 μM auxin indicated a stress response. In addition, A total of 176 *TabZIP* genes were identified from the wheat genome and gene structure and protein motif analyses indicated that closely clustered *TabZIP* genes were relatively conserved within each subgroup. There are 4 *TabZIPs* were downregulated in response to 1 μM auxin, 17 *TabZIPs* were downregulated and 4 *TabZIPs* were upregulated in response to 50 μM auxin through the transcriptome data. These auxin-responsive *TabZIP* genes may be used as candidate genes for root regulation.

Conclusions

The results revealed that the transcriptomes underlying the root regulation in response to these two auxin concentrations were different. These findings provide a comprehensive molecular framework of the auxin regulatory network as well as potential key genes for improving the wheat root system to optimize its absorption of water and nutrients, and finally improve wheat quality and yield.

Background

Auxin is involved in many critical aspects of plant growth especially in regulating root development and physiology, such as the response to gravity and light[1], the formation of lateral roots[2]. The effect of auxin on root growth is related to its concentration. Higher concentration of auxin inhibits the growth of main root and promotes the formation of adventitious root[3].Wheat (*Triticum aestivum*) is one of the most important staple crops that provieds protein and carbohydrates to the human diet. With respect to the increasing global population and the severe impact of climate change, it is of great practical important to optimize the wheat root configuration to increase yields and improve quality. However, because of the inherent difficulties in measuring and assessing the structures of belowground organs, studies tend to focus on aboveground organs and structures[4]. Moreover, the root volume of modern wheat varieties cultivated since the Green

Revolution is much smaller than that of the local original varieties, and such small roots aren't conducive to the effective absorption of water and fertilizer and to the obtainment of the greatest yield[5]. Therefore, the key to the new Green Revolution is the belowground root system, and the improvement to roots will become one of the important breakthroughs in plant science.

Auxin is required for all aspects of root development, genes involved in auxin biosynthesis, transport or signal transduction as well as auxin-responsive genes have great effects on root development[3, 6]. GH3 genes are a family of auxin-driven early response genes that act to regulate the auxin pool. Activation of OsGH3.13 reduces the auxin content to enhance drought tolerance in rice and alters root architecture [7, 8]. Within the LAX family of auxin influx carriers, AUX1, LAX2, and LAX3 are induced in roots by auxin treatment[9]. The Aux/IAA genes which repress Auxin Response Factors (*ARFs*) activity at low cellular auxin concentrations have been used as marker genes for auxin-dependent transcription[10, 11]. Morever, expression of auxin-responsive genes involve the interactions between *cis*-acting DNA sequence elements and *trans*-acting transcriptional regulators[6]. In general, the transcriptional response to auxin is primarily mediated through cis-regulatory AuxREs[12]. Recent research has proposed that, in addition to *ARF*s that bind AuxREs, some members of the basic leucine zipper (*bZIP*) TF family are involved in the transcriptional control of auxin-regulated genes via *bZIP* response elements (*ZRE*s) [13]. Whereas *bZIP*-binding sites are not sufficient to mediate auxin response themselves, they couple to AuxREs and enhance auxin-mediated transcription of a GH3 gene in an auxin concentration-dependent manner[14]. Morever, BZI-1/BZI-2 heterodimers in Tobacco function as modulators of auxin-mediated transcription which are most likely to be dependent on the well-defined auxin response circuit controlled by ARFs[15].

The *bZIP* family is one of the largest and most diverse TF families, and its members are involved in seed germination, light signalling, hormone and sugar signalling[16, 17]. *bZIP* proteins are characterized by a conserved *bZIP* domain, which is 60 to 80 amino acids in length and has two distinct structures[18, 19]. The first structure is a highly conserved basic DNA-binding region comprising 16 amino acid residues, and the most striking characteristic is the presence of an invariant N-x7-R/K motif. The other structure is a more diversified leucine zipper dimerization region. It has been thoroughly studied in a variety of biological systems. Humans have 56 *bZIP* proteins[20], whereas there are a total of 77 *AtbZIP* genes[21] and 89 *OsbZIP* genes[18]. The role of some *bZIP* genes in the regulation of specific auxin response has been preliminarily studied. VIP1 is a *bZIP* TF in Arabidopsis which changes root cap structures and local auxin responses, and decreases the root vertical growth index (*VGI*)[22]. In addition, the HY5 gene, which contain *bZIP* domain, is involved not only in the light response but also in gravitropic and secondary thickening, in which auxin plays an important role[23, 24]. OsbZIP46 exhibits an auxin response, suggesting a possible role of OsbZIP46 in mediating cross-talk between abscisic acid (ABA) and indoleacetic acid (IAA) in rice[25]. Although studies on the role of *bZIP* TFs in the regulation of auxin are limited, it would be of great importance to understand the various roles of *bZIP* family members and their structures for further investigation of the molecular mechanisms of auxin involved in root regulation.

Transcriptomic analysis is an effective method for global expression profiling of genes involved in the response of auxin in plants, and compared with microarrays, RNA-seq can provide more information at a more affordable cost and is emerging as a powerful tool for transcriptomic analyses[26]. There have been more comprehensive studies on the time effect and tissue specificity of single concentrations of auxin. However, in

our work, we focused on the effects of different auxin concentrations (1 μM and 50 μM) on transcriptomic differences in wheat roots in order to reveal the similarities and differences of molecular networks of wheat roots in response to different concentrations of auxin. Furthermore, we made a comprehensive bioinformatics analysis of the *TabZIP* genes from the wheat genome. Phylogenetic and conserved motif analyses were performed to reveal the differences among subgroups of *TabZIP* genes. Additionally, *TabZIP* genes involved in auxin response were found from the transcriptome data, as well as the expression differences of these auxin- responsive *TabZIP* genes under different concentrations were compared and analyzed. Subsequently, we discuss the relationship of these auxin-responsive *TabZIP* genes in gene structures and functional characteristics to reveal their potential role in the auxin regulatory network. The results of this study provided the basis for further study of *TabZIP* genes and provided some promising candidate genes for transgenic technology to improve the root system of wheat.

Results

Phenotypic responses to different concentrations of auxin in wheat roots

The seedlings with the same growth rate(Fig. 1a) were selected for treatments with different concentrations of auxin (1 μM and 50 μM). Fig. 1b shows the changes in the appearance of wheat leaves and roots affter 1-week treatments**.** Compared with control, the leaves of wheat treated with 1 μM auxin didn't show significant difference, however, the length of its' seminal root was much shorter. This indicated that 1 μM auxin significantly inhibited root growth but had little effect on the growth of leaves. In response to 50 μM, significant changes had taken place in both leaf and root tissues. The leaves and the length of the seminal roots were shorter than both 1 μM and contorl. The data in Fig. 1d show there are significant differences in the root length of wheat samples under the different treatments. The effects of these different concentrations of auxin are reflected by the wheat phenotype, and significant genetic changes took place at the same time.

Overview of libraries data sets by RNA-seq

As shown in Table 1, a total of 100.78G nucleotides, equivalent to 686,382,894 raw reads and 678,304,326 clean reads were generated from the libraries, an average of 75 million reads (11.2 Gb) per sample. The size of data greatly exceeded the transcript size of the wheat genome, therefore, it was assumed to cover most transcribed genes within the wheat genome. The percentage of clean reads with a Q30 was greater than 89% for all nine of the samples, and the GC content ranged from 53.11 to 53.71%. After aligning the nine sets of clean reads to the reference genome (TAGCv1) individually, the percentage of reads mapping to the reference genome ranged from 88.31 to 92.36%, with uniquely matches were from 81.46 to 85.25%. In summary, the sequencing quality of the nine samples was high and suitable for follow-up analysis.

Overview of the data and identification of differentially expressed genes (DEGs)

The results showed that 9783 genes were classified as DEGs. The expression of most of these genes was down-regulated in the two treatments (Fig. 1e). There were 308 and 326 genes whose expression was upregulated and downregulated, respectively, were identified under 1uM auxin treatment (Additional file 1: TableS1). There were 6118 genes whose expression was downregulated and 2333 genes whose expression was upregulated in response to 50 μM (Additional file 2: Table S2). As shown in Fig. 1e, there were several

overlapping genes among the DEGs in the two treatments. We performed a Gene Ontology (GO) enrichment analysis to investigate the distribution of DEGs in terms of their involvement in biological process (BPs), cellular components (CCs) and molecular functions (MFs). Twenty-three GO terms (MF, 6 terms; CC, 6 terms; BP, 11 terms) were significantly enriched in the 1 μM auxin treatment compared with the control, and catalytic activity, cell part and metabolic process were the most significantly enriched terms in the MF, CC, and BP categories, respectively (Fig. 2a). In addition, as shown in Fig. 2b, the number of GO terms in the 50 μM auxin treatment increased to 34 (MF, 11 terms; CC, 9 terms; BP, 14 terms). The most significantly enriched terms in the three categories were the same between the two treatments.

To investigate the major pathways of the DEGs, we aligned all the DEGs to Kyoto Encylcopedia of Genes and Genomes (KEGG) pathways (Additional file 3: Table S3 and Table S4). In response to 1 μM auxin, the DEGs were enriched in 42 pathways, in which glycolysis/gluconeogenesis (6 DEGs) and glutathione metabolism (4 DEGs) were the top two pathways containing the greatest number of DEGs (Fig 3a. Q-value < 0.05). In response to 50 μM auxin, thirty-six KEGG pathways were identified (Fig. 3b) and the top three pathways were phenylpropanoid biosynthesis (56 DEGs), plant-pathogen interaction (45 DEGs) and photosynthesis (39 DEGs). As shown in Fig. 3a, b, different enriched pathways were identified in the two different treatments, with the exceptions of the insulin signalling and MAPK signalling pathway-plant pathways (Q-value < 0.05).

In total, 3279 DEGs were clustered into 8 profiles by Short Time-series Expression Miner software (STEM, Fig. 4a). The general trend diagram of all profiles is shown in Figure S1 (Additional file 4). Of the 3279 DEGs, 2831 were further clustered into 3 profiles (Fig. 4b-d, p-value $\leq$0.05), which involved two downregulated patterns (profile 1 and profile 0) and an upregulated pattern (profile 6). Profile 1 and profile 0 contained 1743 and 602 DEGs, respectively, while profile 6 contained 486 DEGs. Of the DEGs, 19.18% (629/3279) were annotated. The top 20 KEGG pathways with the highest representation of the DEGs are shown in Table 2. The ribosome (ko03010), starch and sucrose metabolism (ko00500), plant hormonesignal transduction (ko04075), phenylpropanoid biosynthesis (ko00940), photosynthesis (ko00195), and carbon metabolism (ko01200) pathways were significantly enriched. However in profile 6, no DEGs were annotated to ribosome pathway. The starch and sucrose metabolism pathway was the second most enriched pathway, and 5 DEGs that accounted for 7.69% of 65 DEGs in profile 6 were annotated to this pathway.

The wheat genome contains 176 *TabZIP* transcription factors.

A total of 468 sequences (including splice variants) were identified on the basis of the functional annotation (PFAM domains) of the TGAC wheat genome. This dataset was simplified by keeping only one splice variant from each genomic locus for further analyses (Additional file 5: Table S5). A total of 185 sequences were identified by the SMART, PFAM and CDD programs. To facilitate the analysis and understanding of evolutionary trees, we used a consistent naming pattern for all *TabZIP* genes, taking into account their subfamily association, phylogenetic relationships and subgenomic location. Each gene name starts with an abbreviation for the species name, e.g., *Triticum aestivum* (Ta). The gene names include A, B or D, indicating the chromosomes on which they are located, as shown in Table S5 (Additional file 5). *AtbZIP* TFs have been classified into 10 groups based on the sequence similarity of basic regions and certain conserved motifs[16]. Similarly, *OsbZIP* TFs have been classified into 11 groups (I–XI) on the basis of their amino acid sequences and DNA-binding sites within the *bZIP* basic domain[18]. Domain analysis revealed that all but five of the

potential *TabZIP* TFs had a typical *bZIP* domain with an invariant N-x7-R/K motif within the basic region and a heptad repeat of Leu or other bulky hydrophobic amino acids (Ile, Val, Phe, or Met) positioned exactly nine amino acids upstream of R/K toward the C-terminus. Of the remaining five, in the case of TabZIP4A_73, TabZIP4D_91, TabZIP5A_95 and TabZIP5D_119, the conserved Arg/Lys in the basic region was replaced with an Ile residue. In the case of TabZIP3A_51, the conserved Arg/Lys in the basic region was replaced with a Cys residue[27]. When generating the unrooted neighbour-joining phylogenetic tree via MEGA 7, the short sequences of TabZIP1A_1, TabZIP2B_29, TabZIP2B_30, and TabZIP3B_62 were artificially eliminated, and a total of 176 *TabZIP* genes were ultimately determined.

Gene structure, motif composition, and phylogenetic classification analysis of *TabZIP* genes

To analyse the evolutionary relationships among the *bZIP* family members in wheat, Arabidopsis and rice, 196 amino acid sequences were used to construct a phylogenetic tree. Recently, studies have reported that the *bZIP* TFs from Arabidopsis and rice are divided into 10 and 11 major clades, respectively, each of which contains more than 12 members (multi-gene clades), 4 to 10 members (medium-gene clades), or 1 to 3 members (oligo-gene clades)[16, 28]. *bZIP* domains of 10 different *AtbZIP* genes and 10 different *OsbZIP* genes (Additional file 5: Table S6) from each of the subgroups were selected as representatives for further comparison [16, 18]. All sequences information is shown in Table S6. Based on the phylogenetic relationships and gene structure information obtained here, *TabZIP* family can be divided into 9 groups (1–9, Fig. 5). Gene phylogenetic classification plays an important role in the evolution of multiple gene families[29].

Gene structural diversity is an vital component of gene family evolution and further supports phylogenetic groupings[30]. The intron/exon organization and number of introns are typical imprints of gene evolution within gene families[31]. The percentage of intronless *TabZIP* family members obtained in the present study was 18.75%, which was similar to that in rice (19.1%[18]); TabZIPU_185 in group 3 had the highest number of introns (9). Most *TabZIP* genes contained less than 5 introns (Fig. 7). Generally, closely clustered *TabZIP*s in the phylogenetic tree exhibited similar exon-intron structures, including those for exon length and intron numbers. The multi-gene clades included groups 1, 5, 7, 8, and 9. Most intronless *TabZIP*s clustered into group 8, except for TabZIP7D_174, whose motif position obviously differed from that of the other genes in the same group. The structure of genes in group 8 is more compact than that of genes in group 5, and the group 5 genes have one intron. Oligo-gene clades include groups 3 and 6, which contain seven to nine introns.

To further investigate the structural features of *TabZIPs*, the 196 *bZIP* protein sequences were analysed using the Multiple Expectation maximization for Motif Elicitation (MEME) tool, which revealed 10 conserved motifs (Fig. 7). The features of these protein motifs are listed in Additional file 5: Table S7. Motif 2 was present within the *TabZIP*s in most groups, indicating evolutionary conservation. Compared with group 9, whose motifs are more numerous and complex, group 1 is characterized by the presence of motif 1. Motif 9 of groups 3, 7, and 8 indicates that the proteins have a longer Leu zipper. Most of the closely related members showed similar motifs in terms of alignment and position indicated that they may possess similar biological functions. Overall, the conserved motif compositions and similar gene structures of the *TabZIP* members within the same group, together with the phylogenetic analysis results, strongly support the reliability of the group classifications.

To further elucidate the phylogenetic mechanisms of *TabZIP* family, we constructed comparative syntenic maps of wheat together with Arabidopsis and rice(Fig. 6a). A total of 14 and 130 *bZIP* genes showed syntenic relationships with those in Arabidopsis and rice respectively, suggesting that *TabZIPs* were more closely allied with *OsbZIPs* than *AtbZIPs* and that the large-scale expansion of these families may not have occurred before the monocot-dicot split[32]. Importantly, related studies of *OsbZIPs* can also provide a theoretical basis for *TabZIP* family.

Differential expression of *TabZIP* genes in different auxin concentration treatments

The fragments per kilobase of transcript per million mapped reads (FPKM) values of the 22 *TabZIP* genes are listed in Additional file 5: Table S8, and a hierarchical clustering analysis and heatmap were generated to display the expression patterns of the *TabZIP* genes (Fig. 8a). There were only four *TabZIP* genes (TabZIP6B_141, TabZIP6D_147, TabZIP7A_158, and TabZIP7D_169) changed in response to 1 μM auxin, and the expression of them was downregulated. In addition, each has 3 introns. TabZIP7A_158 in group 9 didn't respond to 50 μM auxin, but the expression of TabZIP6B_141, TabZIP6D_147 and TabZIP7D_169, which contain a common motif 4 in group 4, remained downregulated in response to 50 μM auxin. The expression of the TabZIP6B_141 and TabZIP6D_147 parallel pair was downregulated to a great extent under 50 uM than under 1 μM, while TabZIP7D_169 was downregulated to a similar extent under the two concentrations. 18 of the 22 *TabZIP* genes did not respond to 1 μM auxin; their expression changed only in response to 50 μM auxin, with the expression of 4 and 14 upregulated and downregulated, respectively. With the exceptions of TabZIP1D_15, whose expression was upregulated, and TabZIP1A_5, whose expression was downregulated, all of the 18 TabZIP genes contain motif 2. The genes whose expression was upregulated were concentrated in groups 1, 5, and 6, but there were also genes whose expression was downregulated in group 5. The expression of TabZIP7B_161 and TabZIP7B_167 decreased the most. Moreover, the genes whose expression was downregulated showed a more complicated motif composition than did the genes whose expression was upregulated, and their intron number was more varied.

Validation of differential transcription using quantitative real-time PCR (qRT-PCR)

To further verify the findings from Illumina RNA-Seq results, we have performed 9 DEGs for their key roles in response to different concentrations of auxin by qRT-PCR. According to the response results of *TabZIPs* to different concentrations of auxin and the grouping of *TabZIPs*, we first selected 15 representative *TabZIPs* to enhance the reliability of the results by qPCR, but the amplification effect of 6 of them was not good, and finally the results of 9 *TabZIPs* were obtained(Fig. 8b). Although TabZIP6B_141, TabZIP6D_147, TabZIP5B_118, TabZIP6A_134 and TabZIP7A_158 were down-regulated at different auxin concentrations, TabZIP6B_141 and TabZIP6D_147 were down-regualated much more under 1uM treatment than 50 uM treatment, TabZIP5B_118 was down-regualated much more under 50uM treatment than 1 uM treatment. TabZIP5A_103, TabZIP5D_130 and TabZIPU_182 only responded specifically under 50uM. Most of qPCR outcomes correlated closely with the transcriptomic results calculated from the RNA-Seq output indicated that these genes are indeed involved in the auxin response.

Discussion

Effects of inhibitory concentrations and stress concentrations of auxin on wheat roots

Treatments with exogenous auxin can ablate root elongation, induce lateral root formation, and globally affect the levels of transcripts[33, 34]. Our data concerning two auxin concentrations that showed 1uM auxin had an inhibitory effect on wheat roots, while 50 μM auxin caused a stress response. Many auxin-induced physiological or molecular changes that occurred in the two treatments differed, suggesting the importance of the concentration effects of auxin. Here, we analysed the inhibitory concentration (1 μM) and stress-concentration (50 μM) effects of auxin on the biology of and molecular processes in wheat roots.

With respect to inhibitory-concentration effects, we found that relatedly few genes responded to 1 μM auxin, and only 7.57% (48/634) of the genes were significantly enriched in KEGG pathways. Glycolysis/gluconeogenesis (6 DEGs) and glutathione metabolism (4 DEGs) were the top two enriched KEGG pathways (Fig. 2c), indicating that these DEGs are relatively highly sensitive to the treatment with inhibitory concentrations. The expression of most of these 10 DEGs was downregulated by auxin treatment. At inhibitory concentrations, auxin inhibits H^+-ATPases and causes alkalinization of cell walls. A relatively high pH of the apoplast decreases the activity of expansins and endotrans glucosylases/hydrolases and increases peroxidase activity, cross-linking hydroxyproline-rich glycoproteins and counteracting cell wall-loosening enzymes[35, 36]. Many of these enzymes are associated with plant defence mechanisms in response to biotic or abiotic stress[37]. Moreover, genes involved in glutathione reaction are essential enzymes in plant stress resistance and protect tissues against oxidative stress, toxins, herbicide stress, and other stressors[38].

With respect to stress-concentration effects, we observed that high levels of auxin cause plant stress, which involves inducing the expression of defence- and detoxification-related genes to maintain auxin homeostasis. Phenylpropanoid biosynthesis (56 DEGs), plant-pathogen interaction (45 DEGs) and photosynthesis (39 DEGs) were the top enriched KEGG pathways (Fig. 3b). The expression of most genes enriched in the plant-pathogen interaction pathway was strongly upregulated in response to auxin treatment. This pathway in profile 6 was the most enriched, which implies that there are specific response mechanisms to very high auxin concentrations. These responses are possibly an adaptation to pathogen infection. In addition, the phenylpropanoid pathway is one of the pathways for lignin biosynthesis in plants, and its stimulation is considered a common feature of several abiotic stress responses[39]. Lignin is the main component of both the cell wall and apoplastic barriers and is the main structure in plant mechanical support and defence systems[40]. Therefore, it could be suggested that high concentrations of auxin may stimulate the phenylpropanoid pathway in wheat roots, leading to a shift in metabolism toward lignin.

Auxin signals interact with many pathways involved in wheat root growth

The plant root is a dynamic structure which is constantly modified in a temporal and spatial manner to respond to environmental stimuli including auxin[41]. Auxin had a relatively strong effect on the expression of genes annotated as participating in ribosome and hormone-dependent signalling pathways (Table 2). Ribosomal proteins are known translational regulators of the auxin response and provide downstream regulation of lipid-based metabolic processes involved in tissue differentiation and transport[42]. This activity is essential in the developing meristem for the specificity of root stem cells. In addition, evidence for the cross-

talk between auxin and light signalling[43] and sugars[44] is growing. An enrichment of genes involved in the response to photosynthesis was observed in response to treatment with auxin. Because of the complexity of the hormone-light interaction effect in root development, additional advances in our understanding of hormonal regulation of the root genome may benefit from the utilization of dark-grown root systems[45]. These investigations may find direct changes related to belowground development processes by removing the changes in chloroplast-related processes. In Arabidopsis, mutations in two members of a family of 19 GH3-related proteins provide further evidence for the proposed link between auxin signalling and photomorphogenesis[43, 46]. Moreover, the quantitative level of GH3 transcription has been shown to be regulated by *bZIP* TFs via G-boxes. Our study implicates several core pathways and *TabZIP* genes as being involved in auxin stimulation, may revealing the dynamic regulatory process of auxin in the wheat root system.

Evolutionary relationships and gene structure analyses of the TabZIP gene family can provide information for the study of specific functions

bZIP TFs invole in the light response, the stress response and sucrose signalling, pathogen defence, seed maturation and flower development[17]. Within the DNA cis-acting elements preferentially bound by *bZIP* TFs, the G-box element is ubiquitous in genes induced by ABA, auxin, rosin and salicylic acid[17, 47]. Here, we identified 176 *TabZIP* genes, which we assigned to 9 conserved subfamilies (Fig. 5). The gene structures and protein motifs were relatively conserved in the groups, which provided a valuable reference for *TabZIPs*' analysis and function(Fig. 7). Most of the paralogous pairs had the same exons and motifs; however, some pairs had different numbers of exons but had the same motifs (exons 2 and 5 in TabZIP7D_171 and TabZIPU_179, respectively, and exons 7 and 9 in TabZIPU_185 and TabZIPU_178, respectively). This may be due to the loss or gain of exons during gene evolution[32]. The differences in gene structure and additional conserved motifs among the different groups may be related to the functional diversity of *TabZIP* genes.

Functional characterization and elucidating the roles of auxin-responsive TabZIP genes in auxin regulatory networks

The distribution of *TabZIPs* that responded to different concentrations of auxin was not concentrated, indicating that they may play an key role in different mechanisms. Under 1 μM auxin, which exerted an inhibitory effect on the roots, there were only 4 *TabZIP*s whose expression was down-regulated, while under 50 μM auxin, the number of down-regulated *TabZIP*s increased, and there were 4 *TabZIP*s whose expression was up-regulated. By combining gene structures, phylogenetic and synteny analysis, new clues to the biological function of *TabZIP* genes could be inferred through comparison with those function-known *bZIP* genes from model plants. Of the 4 genes that responded to 1 μM auxin, 3 genes (TabZIP6B_141, TabZIP6D_147, and TabZIP7D_169) were from group 4 and classified with AtbZIP5G_H (or HY5 TFs). TabZIP6B_141 and TabZIP6D_147 have also been described as homologues of HY5 and they are already sensitive to 1uM auxin (Fig. 8a). The structure of these proteins has a relative long leucine zipper region and contains two Asn residues. Interestingly, HY5 TFs are involved in the light-based regulation and likely play a role in a wide variety of stimulus responses and developmental processes in the hypocotyl and roots[23, 48]. The expression of TabZIP5A_103 and TabZIP5D_130, which are classified together with AtbZIP4G_G and OsbZIP01g_10 (*OSBZ8*) in group 6, were upregulated under 50 μM auxin. In Arabidopsis, AtbZIP16 and

AtbZIP68 in group G can form homodimers and heterodimers with GBF1, GBF2 and GBF3 to regulate light-responsive promoters[49–52]. GBF1/GBF2 is involved in the regulation of plant morphogenesis in response to blue light, which promotes the expansion of cotyledons and the formation of lateral roots[53]. OsbZIP01g_10 was shown to have structural features typical of the GBF-type *bZIP* proteins[54]. Therefore, *TabZIP* genes may play an important role in root growth in response to auxin cross-talk with light signals. But we should also consider the influence of hydroponics on the results, passive exposure of the roots to light may strongly activate photosynthesis in root tissues. *TabZIP*s in both group 5 and group 6 contain only motif 2, indicating that their genetic relationships are relatively close. However, the members in group 5 are diverse. The expression of TabZIP2D_38 was upregulated in response to 50 μM auxin, while the expression of TabZIPU_182, TabZIP2D_37 and TabZIP7B_161 in group 5 was downregulated. Moreover, the function of ATbZIP3G_B, which is in the same group, is unknown, indicating that there may be other unknown genes in this group, or the function of this protein may be similar to that of group 6 proteins. TabZIP2D_38, TabZIPU_182 and TabZIP7B_161 are in the same subgroup as OsbZIP02g_6. Therefore, there isn't enough evidence on which to speculate their function.

TabZIP genes that are highly homologous to AtbZIP5G_C in Arabidopsis group C and AtbZIP1G_S in groupS were divided into group 7 and group 8. The group S genes tend to heterodimerize within the subgroup or with group C bZIP genes in Arabidopsis, dimerisation is likely to fulfil specific functions in gene regulation[55, 56]. Members of these groups have markedly expansive leucine zipper regions with up to nine heptapeptide repeats. *AtbZIP11* which was in the C/S *bZIP* low-energy activated network gained control over the root meristem by directly activating IAA3/SHY2 transcription[57]. Morever, *bZIP11* modulate Aux/IAA and GH3 expression by recruiting the histone acetylation (HAT) machinery to target promoters[58]. Additionaly, genes in group 8 contain almost no introns, whereas the expression of individual genes in groups 7 and 8 was downregulated in response to 50 μM auxin. In previous studies, genes with few or no introns were thought to display enhanced levels of expression in plants[59, 60]. To respond in a timely manner to various stresses, genes with a compact genetic structure with relatively few introns would be rapidly activated[61]. These genes may be involved in different reaction processes, homologues of group S bZIPs are also transcriptionally activated after stress treatment (e.g. cold, drought, wounding)[62]. In rice, LIP19 and OsOBF which are classified with OsbZIP12g_8 interact in response to cold stress[63].

There are also some genes whose expression was downregulated under 50 μM auxin in group 9, and they may complement or replace TabZIP7A_158 in the same group, whose exprsesion was downregulated under 1 μM auxin. The *TabZIP*s in group 9 were homologous to those in Arabidopsis group A (AtbZIP2G_A) and OsbZIP08g_5 (*TRAB1*). 7 *AtbZIP* genes in group A (such as *AtbZIP39*/*ABI5* and *AtbZIP36*/*ABF2*/*AREB1*) and OsbZIP08g_5 (*TRAB1*) were studied, the available functional information suggests they play roles in the response to ABA or stress signalling, including drought and salinity[54, 64–66]. TabZIP6A_134 was described as homologues of *ABI5*. Interestingly, *ABI5* probably acts by recruiting the B1 domain of the *ABI3* protein to the LEA promoter. *ABI3* transcription may be regulated by auxin, and auxin signalling in lateral root development may have an ABI3-dependent component[67]. Moreover, *ABI3* TFs could potentially interact with other *ARF* or *IAA* proteins to mediate auxin responses[68, 69]. As discussed above, many *TabZIPs* probably have overlapping functions, Our identification of all *TabZIP* genes is thus a necessary prerequisite for the dissection of individual *bZIP* protein function. Further investigation of the molecular mechanisms underlying

how *TabZIP*s perceive auxin stimulus-induced signals and how *TabZIP*s control the expression of target genes will unravel the role *TabZIP*s play in root development and the auxin signalling pathways in wheat.

Conclusion

Transcriptomic studies of wheat roots were carried out to compare their physiological and transcriptional responses to different concentrations of auxin. Our results showed that different auxin concentrations had different effects on roots' genes of wheat. The inhibitory effect of 1 μM auxin on roots manifested as an enrichment of the glycolysis/gluconeogenesis and glutathione metabolism pathways. Enrichment of the phenylpropanoid biosynthesis and plant-pathogen interaction pathways in response to 50 μM auxin indicated a stress response. Plant hormone signal transduction, starch and sucrose metabolism and photosynthesis were enriched in all the profiles. Furthermore, *TabZIP* TFs in respond to different concentrations of auxin was also detected. The gene structure and phylogenetic classification analysis of *TabZIPs* further confirmed that the complexity of the regulatory machinery involved in different concentrations of auxin and cross-regulation of multicomponent signalling pathways. Determining which of these *TabZIPs* are the primary responses of different cincentrations auxin is necessary before the molecular basis can be fully described. Such genes would represent candidates for interfering in wheat root regulation.

Methods

Plant Materials, Growth Conditions and Auxin Treatments

The wheat (*Triticum aestivum*) variety used in this study is "Chinese Spring" which is sequenced and used worldwide, and seeds are obtained from our Lab. The wheat seeds were surface sterilized with 1% NaClO solution for 15 min, rinsed three times with distilled water, kept at 4 ℃ for 2 days, and then transferred in to growth chamber (14/10 h day/night photoperiod under 24/17 ℃ day/night temperatures). After 1 days, 30 healthy seedlings with approximately equal root lengths were transferred to Hoaglands containing different concentrations of auxin (0, 1, 50 uM). After 1 week, images were photographed, and the root elongation was measured by NIH-Image software (https://imagej.nih.gov/ij/index.html). Meanwhile, Roots were collected for transcriptomic and qRT-PCR analysis.

mRNA sequencing by Illumina HiSeq

Total RNA of each sample was extracted using TRIzol Reagent (Invitrogen) / RNeasy Mini Kit (Qiagen) / other kits. Total RNA of each sample was quantified and qualified by Agilent 2100 Bioanalyzer (Agilent Technologies, Palo Alto, CA, USA), NanoDrop (Thermo Fisher Scientific Inc.) and 1% agrose gel.1 μg total RNA with RIN value above 7 was used for following library preparation. Next generation sequencing library preparations were constructed according to the manufacturer's protocol (NEBNext® Ultra™ RNA Library Prep Kit for Illumina®).

The poly(A) mRNA isolation was performed using NEBNext Poly(A) mRNA Magnetic Isolation Module (NEB) or Ribo-Zero™ rRNA removal Kit (illumina). The mRNA fragmentation and priming was performed using NEBNext First Strand Synthesis Reaction Buffer and NEBNext Random Primers. First strand cDNA was synthesized using ProtoScript II Reverse Transcriptase and the second-strand cDNA was synthesized using

Second Strand Synthesis Enzyme Mix. The purified double-stranded cDNA by AxyPrep Mag PCR Clean-up (Axygen) was then treated with End Prep Enzyme Mix to repair both ends and add a dA-tailing in one reaction, followed by a T-A ligation to add adaptors to both ends. Size selection of Adaptor-ligated DNA was then performed using AxyPrep Mag PCR Clean-up (Axygen), and fragments of ~360 bp (with the approximate insert size of 300 bp) were recovered. Each sample was then amplified by PCR for 11 cycles using P5 and P7 primers, with both primers carrying sequences which can anneal with flow cell to perform bridge PCR and P7 primer carrying a six-base index allowing for multiplexing. The PCR products were cleaned up using AxyPrep Mag PCR Clean-up (Axygen), validated using an Agilent 2100 Bioanalyzer (Agilent Technologies, Palo Alto, CA, USA), and quantified by Qubit 2.0 Fluorometer (Invitrogen, Carlsbad, CA, USA).

Then libraries with different indices were multiplexed and loaded on an Illumina HiSeq instrument according to manufacturer's instructions (Illumina, San Diego, CA, USA). Sequencing was carried out using a 2x150 bp paired-end (PE) configuration; image analysis and base calling were conducted by the HiSeq Control Software (HCS) + OLB + GAPipeline-1.6 (Illumina) on the HiSeq instrument. The sequences were processed and analyzed by GENEWIZ.

De novo assembly of RNA-seq reads and quantifying gene expression

In order to remove technical sequences, including adapters, polymerase chain reaction (PCR) primers, or fragments thereof, and quality of bases lower than 20, pass filter data of fastq format were processed by Trimmomatic (v0.30) to be high quality clean data. The obtained quality filtered reads were de novo assembled into contigs by the Trinity Program[70]. Unigenes were defined after removing redundancy and short contigs from the assembly. Reference genome sequences and gene model annotation files of relative species were downloaded from genome website, such as UCSC, NCBI, ENSEMBL. Secondly, Hisat2 (v2.0.1) was used to index reference genome sequence. Finally, clean data were aligned to reference genome via software Hisat2 (v2.0.1). The number of unique-match reads was calculated and normalized to RPKM (reads per kb per million reads) for gene expression analysis. Differential expression analysis used the DESeq Bioconductor package, a model based on the negative binomial distribution. After adjusted by Benjamini and Hochberg's approach for controlling the false discovery rate, p-value of genes were setted <0.05 to detect differential expressed ones[71]. The differentially expressed genes (DEGs) between control and 1uM, or between control and 50uM, or between 1uM and 50 uM were restricted with FDR (false discovery rate)≤0.001 and the absolute value of log2 Ratio≥1. To examine the expression profile of DEGs, the expression data υ (from Control, 1uM and 50uM treatment) were normalized to 0, log2 (υ1uM/υControl), log2 (υ50uM/υControl). and then clustered by Short Time-series Expression Miner software (STEM)[72]. GO-Term Finder was used identifying Gene Ontology (GO) terms that annotate a list of enriched genes with a significant p-value less than 0.05 and we used scripts in house to enrich significant differential expression gene in KEGG pathways.

Sequence retrieval and annotation of *TabZIP* TFs

The protein sequence datas of wheat were download from the Ensembl Plants (http://plants.ensembl.org/index.html). Functional annotations were filtered for PFAM (http://pfam.xfam.org/) [73] identifiers of the *bZIP_1*, *bZIP_2* and *bZIP_C* (PF00170, PF07716, and PF12498), respectively. HMMER 3.0 (http://eddylab.org/software/hmmer/Userguide.pdf) was used to search the *bZIP*

genes from wheat genome database. A total of 468 sequences were identified. The default parameters were adopted and the cutoff value was set to1.2e-09 to screen 230 sequences. Splice variants were excluded and only the first variant was kept for further analysis, with seven exceptions. All candidate genes that may contain *bZIP* domain based on HMMER results were further examined by confirming the existence of the *bZIP* core sequences using the SMART, PFAM and CDD program. Finally, Each potential gene was then manually examined to ensure the invariant N-x7-R/K motif in the basic region and a heptad repeat of Leu or other bulky hydrophobic amino acids (Ile, Val, Phe, or Met) positioned exactly nine amino acids upstream of R/K toward the C terminus. There are 176 sequences were identified.

Phylogenetic Analysis and Classification

Presently, the *AtbZIP* TFs have been classified into 10 groups [16] and *OsbZIP* TFs have been classified into 11 groups (I–XI) [18]. Using JGI database website (https://phytozome.jgi.doe.gov/pz/portal.html) search and download protein sequences of the *bZIP* TFs of rice and Arabidopsis. *AtbZIP* and *OsbZIP* from each of the groups or subgroups, were selected as representatives for the further comparison. Next, the *bZIP* protein sequences of the characterized *bZIP* proteins were used to create multiple protein sequence alignments using ClustalW with default parameters. MEGA7[74] was used to generate the unrooted Neighbor-joining phylogenetic tree with the following parameters: 1000 times bootstrap test, poisson model and pairwise deletions. The classifications of *TabZIP* proteins were based on the topology and bootstrap values of the phylogenetic tree.

Gene Structure and Conserved Motif Characterization

The exon-intron organization of *TabZIP* TFs were determined by comparing predicted coding sequences with their corresponding full-length sequences using the online program Gene Structure Display Server (GSDS: http://gsds.cbi.pku.edu.cn/)[75]. The MEME program (http://meme-suite.org/) for protein sequence analysis was used to identify conserved motifs in the identified *TabZIP* proteins[76]. The optimized parameters were employed as the following: the number of repetitions, any; the maximum number of motifs 10; and the optimum width of each motif, between 6 and 100 residues.

Heatmap of *TabZIP* TFs and the orthologous *bZIP* genes obtained from wheat, Arabidopsis and rice.

Expression levels as log2tpm and a heatmap was generated with MEV. Genes were clustered according to their expression using Hierarchical Clustering (metric:Pearson Uncentered, method: complete).Multiple Collinearity Scan toolkit (MCScanX) was adopted to analyze the gene duplication events, with the default parameters. To exhibit the synteny relationship of the orthologous *bZIP* genes obtained from wheat, Arabidopsis and rice, the syntenic analysis maps were constructed using python written by ourselves. Sequence of *AtbZIP* and *OsbZIP* proteins were obtained based on the description in corresponding literatures and downloaded from the phytozome database.

qRT-PCR verification of differential expression

Total RNA was isolated from roots of wheat subjected to the various concentration treatments described above. cDNA was synthesized from 1 μg total RNA using PrimeScript® (TaKaRa, Japan) and an oligo (dT)

primer, according to the manufacturer's instructions. Primers for quantitative real time PCR (qRT-PCR) were designed by Beacon Designer7.9 software (Premier Biosoft, America) listed in Additional file 5: Table S9 and synthesized by Sangon Biotech (Shanghai) Co., Ltd. SYBR based qRT-PCR reactions (TaKaRa, Japan) were performed on ABI StepOnePlus. Each 20 μL qPCR contained 3 μl diluted cDNA, 1ul of each primer, and 10 μl SYBR qPCR master mix (Vazyme, China), and was following the reaction conditions: 95°C/1 min followed by 40 cycles of 95°C/5 s, 60°C/30s, 72°C/30s except for 4 pairs of primers (TabZIP3A_46, TabZIP6B_141, TabZIP6D_147 and TabZIP7A_158) which were annealed at 63°C. At least three biological replicates were performed for each sample. Relative expression levels of the tested reference genes were determined by Ct values and calculated by $2^{-\triangle\triangle Ct}$.

Abbreviations

AuxinREs: Auxin Response Elements. KEGG: Kyoto Encyclopedia of Genes and Genomes. FPKM: Fragments Per Kilobase of transcript per Million mapped reads.

Declarations

Ethics approval and consent to participate

Not applicable

Consent for publication

Not applicable

Availability of data and material

Raw data was deposited in NCBI database under SRA accession: PRJNA644764. (https://www.ncbi.nlm.nih.gov/SRA /PRJNA644764/). Other datas generated or analyzed during this study are included in this article and its additional files.

Competing interests

The authors declare that the research was conducted in the absence of any commercial or financial relationships that could be construed as a potential conflict of interest.

Funding

This work was supported by the National Natural Science Foundation of China (grant numbers 31601383, 41807516); China Postdoctoral Science Foundation Funded Project (grant numbers 2018M643750, 2018M631199). The funding bodies had no role in study design, data collection, analysis and interpretation, decision to publish, or writing of the manuscript.

Authors' Contributions

JW , XT and YF designed the study, performed data analyses and wrote the manuscript. XT carried out the analysis of *TabZIP* genes, YF performed GO and KEGG pathway analysis, XT and ZJ performed qRT-PCR experiments, JW and ZW revised the manuscript. All authors have read and approved the final manuscript.

Acknowledgments

We would like to express our deep gratitude to all the members of our lab for their kindness and assistance with seeds.

Author details

State Key Laboratory of Crop Stress Biology for Arid Areas, College of Agronomy, Northwest A&F University, Yangling, China.

Xinyu Tian, Ziyao Jia, Zhonghua Wang & Jun Wang

State Key Laboratory of Soil Erosion and Dryland Farming on the Loess Plateau, Northwest A&F University, Yangling, China.

Yan Fang

References

1. Buer CS, Muday GK: **The transparent testa4 mutation prevents flavonoid synthesis and alters auxin transport and the response of Arabidopsis roots to gravity and light**. *Plant Cell* 2004, **16**(5):1191-1205.
2. Casimiro I, Marchant A, Bhalerao RP, Beeckman T, Dhooge S, Swarup R, Graham N, Inze D, Sandberg G, Casero PJ *et al*: **Auxin transport promotes Arabidopsis lateral root initiation**. *Plant Cell* 2001, **13**(4):843-852.
3. Wang Y, Zhang T, Wang R, Zhao Y: **Recent advances in auxin research in rice and their implications for crop improvement**. *J Exp Bot* 2018, **69**(2):255-263.
4. Steen EB, Detmer DE: **A vision for future patient records**. *J Am Med Rec Assoc* 1991, **62**(9):48-54.
5. Waines JG, Ehdaie B: **Domestication and crop physiology: roots of green-revolution wheat**. *Ann Bot* 2007, **100**(5):991-998.
6. Chapman EJ, Estelle M: **Mechanism of auxin-regulated gene expression in plants**. *Annu Rev Genet* 2009, **43**:265-285.
7. Chen Q, Westfall CS, Hicks LM, Wang S, Jez JM: **Kinetic basis for the conjugation of auxin by a GH3 family indole-acetic acid-amido synthetase**. *J Biol Chem* 2010, **285**(39):29780-29786.
8. Zhang SW, Li CH, Cao J, Zhang YC, Zhang SQ, Xia YF, Sun DY, Sun Y: **Altered architecture and enhanced drought tolerance in rice via the down-regulation of indole-3-acetic acid by TLD1/OsGH3.13 activation**. *Plant Physiol* 2009, **151**(4):1889-1901.
9. Paponov IA, Paponov M, Teale W, Menges M, Chakrabortee S, Murray JA, Palme K: **Comprehensive transcriptome analysis of auxin responses in Arabidopsis**. *Mol Plant* 2008, **1**(2):321-337.

10. Mockaitis K, Estelle M: **Auxin receptors and plant development: a new signaling paradigm**. *Annu Rev Cell Dev Biol* 2008, **24**:55-80.
11. Nemhauser JL, Hong F, Chory J: **Different plant hormones regulate similar processes through largely nonoverlapping transcriptional responses**. *Cell* 2006, **126**(3):467-475.
12. Ulmasov T, Murfett J, Hagen G, Guilfoyle TJ: **Aux/IAA proteins repress expression of reporter genes containing natural and highly active synthetic auxin response elements**. *Plant Cell* 1997, **9**(11):1963-1971.
13. Heinekamp T, Strathmann A, Kuhlmann M, Froissard M, Muller A, Perrot-Rechenmann C, Droge-Laser W: **The tobacco bZIP transcription factor BZI-1 binds the GH3 promoter in vivo and modulates auxin-induced transcription**. *Plant J* 2004, **38**(2):298-309.
14. Berendzen KW, Weiste C, Wanke D, Kilian J, Harter K, Droge-Laser W: **Bioinformatic cis-element analyses performed in Arabidopsis and rice disclose bZIP- and MYB-related binding sites as potential AuxRE-coupling elements in auxin-mediated transcription**. *BMC Plant Biol* 2012, **12**:125.
15. Bottner S, Iven T, Carsjens CS, Droge-Laser W: **Nuclear accumulation of the ankyrin repeat protein ANK1 enhances the auxin-mediated transcription accomplished by the bZIP transcription factors BZI-1 and BZI-2**. *Plant J* 2009, **58**(6):914-926.
16. Jakoby M, Weisshaar B, Droge-Laser W, Vicente-Carbajosa J, Tiedemann J, Kroj T, Parcy F, b ZIPRG: **bZIP transcription factors in Arabidopsis**. *Trends Plant Sci* 2002, **7**(3):106-111.
17. Lindemose S, O'Shea C, Jensen MK, Skriver K: **Structure, function and networks of transcription factors involved in abiotic stress responses**. *Int J Mol Sci* 2013, **14**(3):5842-5878.
18. Nijhawan A, Jain M, Tyagi AK, Khurana JP: **Genomic survey and gene expression analysis of the basic leucine zipper transcription factor family in rice**. *Plant Physiol* 2008, **146**(2):333-350.
19. Landschulz WH, Johnson PF, McKnight SL: **The leucine zipper: a hypothetical structure common to a new class of DNA binding proteins**. *Science* 1988, **240**(4860):1759-1764.
20. Deppmann CD, Alvania RS, Taparowsky EJ: **Cross-species annotation of basic leucine zipper factor interactions: Insight into the evolution of closed interaction networks**. *Mol Biol Evol* 2006, **23**(8):1480-1492.
21. Correa LG, Riano-Pachon DM, Schrago CG, dos Santos RV, Mueller-Roeber B, Vincentz M: **The role of bZIP transcription factors in green plant evolution: adaptive features emerging from four founder genes**. *PLoS One* 2008, **3**(8):e2944.
22. Tsugama D, Liu S, Takano T: **The bZIP Protein VIP1 Is Involved in Touch Responses in Arabidopsis Roots**. *Plant Physiol* 2016, **171**(2):1355-1365.
23. Oyama T, Shimura Y, Okada K: **The Arabidopsis HY5 gene encodes a bZIP protein that regulates stimulus-induced development of root and hypocotyl**. *Genes Dev* 1997, **11**(22):2983-2995.
24. Laskowski MJ, Williams ME, Nusbaum HC, Sussex IM: **Formation of lateral root meristems is a two-stage process**. *Development* 1995, **121**(10):3303-3310.
25. Tang N, Zhang H, Li X, Xiao J, Xiong L: **Constitutive activation of transcription factor OsbZIP46 improves drought tolerance in rice**. *Plant Physiol* 2012, **158**(4):1755-1768.

26. Vikman P, Fadista J, Oskolkov N: **RNA sequencing: current and prospective uses in metabolic research**. *J Mol Endocrinol* 2014, **53**(2):R93-101.
27. Nantel A, Quatrano RS: **Characterization of three rice basic/leucine zipper factors, including two inhibitors of EmBP-1 DNA binding activity**. *J Biol Chem* 1996, **271**(49):31296-31305.
28. E ZG, Zhang YP, Zhou JH, Wang L: **Mini review roles of the bZIP gene family in rice**. *Genet Mol Res* 2014, **13**(2):3025-3036.
29. Xu G, Guo C, Shan H, Kong H: **Divergence of duplicate genes in exon-intron structure**. *Proc Natl Acad Sci U S A* 2012, **109**(4):1187-1192.
30. Wei Y, Shi H, Xia Z, Tie W, Ding Z, Yan Y, Wang W, Hu W, Li K: **Genome-Wide Identification and Expression Analysis of the WRKY Gene Family in Cassava**. *Front Plant Sci* 2016, **7**:25.
31. Ji L, Wang J, Ye M, Li Y, Guo B, Chen Z, Li H, An X: **Identification and characterization of the Populus AREB/ABF subfamily**. *J Integr Plant Biol* 2013, **55**(2):177-186.
32. Cao L, Lu X, Zhang P, Wang G, Wei L, Wang T: **Systematic Analysis of Differentially Expressed Maize ZmbZIP Genes between Drought and Rewatering Transcriptome Reveals bZIP Family Members Involved in Abiotic Stress Responses**. *Int J Mol Sci* 2019, **20**(17).
33. Ishikawa H, Evans ML: **Novel software for analysis of root gravitropism: comparative response patterns of Arabidopsis wild-type and axr1 seedlings**. *Plant Cell Environ* 1997, **20**(7):919-928.
34. Lewis DR, Olex AL, Lundy SR, Turkett WH, Fetrow JS, Muday GK: **A kinetic analysis of the auxin transcriptome reveals cell wall remodeling proteins that modulate lateral root development in Arabidopsis**. *Plant Cell* 2013, **25**(9):3329-3346.
35. De Cnodder T, Vissenberg K, Van Der Straeten D, Verbelen JP: **Regulation of cell length in the Arabidopsis thaliana root by the ethylene precursor 1-aminocyclopropane- 1-carboxylic acid: a matter of apoplastic reactions**. *New Phytol* 2005, **168**(3):541-550.
36. Staal M, De Cnodder T, Simon D, Vandenbussche F, Van der Straeten D, Verbelen JP, Elzenga T, Vissenberg K: **Apoplastic alkalinization is instrumental for the inhibition of cell elongation in the Arabidopsis root by the ethylene precursor 1-aminocyclopropane-1-carboxylic acid**. *Plant Physiol* 2011, **155**(4):2049-2055.
37. Cosgrove DJ: **Plant expansins: diversity and interactions with plant cell walls**. *Curr Opin Plant Biol* 2015, **25**:162-172.
38. Chen D, Kawarasaki Y, Nakano H, Yamane T: **Cloning and in vitro and in vivo expression of plant glutathione S-transferase zeta class genes**. *J Biosci Bioeng* 2003, **95**(6):594-600.
39. Vanholme R, Morreel K, Darrah C, Oyarce P, Grabber JH, Ralph J, Boerjan W: **Metabolic engineering of novel lignin in biomass crops**. *New Phytol* 2012, **196**(4):978-1000.
40. Vogt T: **Phenylpropanoid biosynthesis**. *Mol Plant* 2010, **3**(1):2-20.
41. Sanchez-Rodriguez C, Rubio-Somoza I, Sibout R, Persson S: **Phytohormones and the cell wall in Arabidopsis during seedling growth**. *Trends Plant Sci* 2010, **15**(5):291-301.
42. Li R, Sun R, Hicks GR, Raikhel NV: **Arabidopsis ribosomal proteins control vacuole trafficking and developmental programs through the regulation of lipid metabolism**. *Proc Natl Acad Sci U S A* 2015, **112**(1):E89-98.

43. Hsieh HL, Okamoto H, Wang M, Ang LH, Matsui M, Goodman H, Deng XW: **FIN219, an auxin-regulated gene, defines a link between phytochrome A and the downstream regulator COP1 in light control of Arabidopsis development**. *Genes Dev* 2000, **14**(15):1958-1970.
44. Nemeth K, Salchert K, Putnoky P, Bhalerao R, Koncz-Kalman Z, Stankovic-Stangeland B, Bako L, Mathur J, Okresz L, Stabel S *et al*: **Pleiotropic control of glucose and hormone responses by PRL1, a nuclear WD protein, in Arabidopsis**. *Genes Dev* 1998, **12**(19):3059-3073.
45. Silva-Navas J, Moreno-Risueno MA, Manzano C, Tellez-Robledo B, Navarro-Neila S, Carrasco V, Pollmann S, Gallego FJ, Del Pozo JC: **Flavonols Mediate Root Phototropism and Growth through Regulation of Proliferation-to-Differentiation Transition**. *Plant Cell* 2016, **28**(6):1372-1387.
46. Nakazawa M, Yabe N, Ichikawa T, Yamamoto YY, Yoshizumi T, Hasunuma K, Matsui M: **DFL1, an auxin-responsive GH3 gene homologue, negatively regulates shoot cell elongation and lateral root formation, and positively regulates the light response of hypocotyl length**. *Plant J* 2001, **25**(2):213-221.
47. Ying S, Zhang DF, Fu J, Shi YS, Song YC, Wang TY, Li Y: **Cloning and characterization of a maize bZIP transcription factor, ZmbZIP72, confers drought and salt tolerance in transgenic Arabidopsis**. *Planta* 2012, **235**(2):253-266.
48. Chattopadhyay S, Ang LH, Puente P, Deng XW, Wei N: **Arabidopsis bZIP protein HY5 directly interacts with light-responsive promoters in mediating light control of gene expression**. *Plant Cell* 1998, **10**(5):673-683.
49. Weisshaar B, Armstrong GA, Block A, da Costa e Silva O, Hahlbrock K: **Light-inducible and constitutively expressed DNA-binding proteins recognizing a plant promoter element with functional relevance in light responsiveness**. *EMBO J* 1991, **10**(7):1777-1786.
50. Kircher S, Ledger S, Hayashi H, Weisshaar B, Schafer E, Frohnmeyer H: **CPRF4a, a novel plant bZIP protein of the CPRF family: comparative analyses of light-dependent expression, post-transcriptional regulation, nuclear import and heterodimerisation**. *Mol Gen Genet* 1998, **257**(6):595-605.
51. Schindler U, Menkens AE, Beckmann H, Ecker JR, Cashmore AR: **Heterodimerization between light-regulated and ubiquitously expressed Arabidopsis GBF bZIP proteins**. *EMBO J* 1992, **11**(4):1261-1273.
52. Armstrong GA, Weisshaar B, Hahlbrock K: **Homodimeric and heterodimeric leucine zipper proteins and nuclear factors from parsley recognize diverse promoter elements with ACGT cores**. *Plant Cell* 1992, **4**(5):525-537.
53. Mallappa C, Yadav V, Negi P, Chattopadhyay S: **A basic leucine zipper transcription factor, G-box-binding factor 1, regulates blue light-mediated photomorphogenic growth in Arabidopsis**. *J Biol Chem* 2006, **281**(31):22190-22199.
54. Nakagawa H, Ohmiya K, Hattori T: **A rice bZIP protein, designated OSBZ8, is rapidly induced by abscisic acid**. *Plant J* 1996, **9**(2):217-227.
55. Wiese A, Elzinga N, Wobbes B, Smeekens S: **A conserved upstream open reading frame mediates sucrose-induced repression of translation**. *Plant Cell* 2004, **16**(7):1717-1729.
56. Ehlert A, Weltmeier F, Wang X, Mayer CS, Smeekens S, Vicente-Carbajosa J, Droge-Laser W: **Two-hybrid protein-protein interaction analysis in Arabidopsis protoplasts: establishment of a heterodimerization map of group C and group S bZIP transcription factors**. *Plant J* 2006, **46**(5):890-900.

57. Weiste C, Pedrotti L, Selvanayagam J, Muralidhara P, Froschel C, Novak O, Ljung K, Hanson J, Droge-Laser W: **The Arabidopsis bZIP11 transcription factor links low-energy signalling to auxin-mediated control of primary root growth**. *PLoS Genet* 2017, **13**(2):e1006607.

58. Weiste C, Droge-Laser W: **The Arabidopsis transcription factor bZIP11 activates auxin-mediated transcription by recruiting the histone acetylation machinery**. *Nat Commun* 2014, **5**:3883.

59. Chung BY, Simons C, Firth AE, Brown CM, Hellens RP: **Effect of 5'UTR introns on gene expression in Arabidopsis thaliana**. *BMC Genomics* 2006, **7**:120.

60. Ren XY, Vorst O, Fiers MW, Stiekema WJ, Nap JP: **In plants, highly expressed genes are the least compact**. *Trends Genet* 2006, **22**(10):528-532.

61. Jeffares DC, Penkett CJ, Bahler J: **Rapidly regulated genes are intron poor**. *Trends Genet* 2008, **24**(8):375-378.

62. Kusano T, Berberich T, Harada M, Suzuki N, Sugawara K: **A maize DNA-binding factor with a bZIP motif is induced by low temperature**. *Mol Gen Genet* 1995, **248**(5):507-517.

63. Shimizu H, Sato K, Berberich T, Miyazaki A, Ozaki R, Imai R, Kusano T: **LIP19, a basic region leucine zipper protein, is a Fos-like molecular switch in the cold signaling of rice plants**. *Plant Cell Physiol* 2005, **46**(10):1623-1634.

64. Choi HI, Hong JH, Ha JO, Kang JY, Kim SY: **ABFs, a family of ABA-responsive element binding factors**. *Journal of Biological Chemistry* 2000, **275**(3):1723-1730.

65. Finkelstein RR, Lynch TJ: **The arabidopsis abscisic acid response gene ABI5 encodes a basic leucine zipper transcription factor**. *Plant Cell* 2000, **12**(4):599-609.

66. Lopez-Molina L, Mongrand S, Chua NH: **A postgermination developmental arrest checkpoint is mediated by abscisic acid and requires the AB15 transcription factor in Arabidopsis**. *Proc Natl Acad Sci U S A* 2001, **98**(8):4782-4787.

67. Brady SM, Sarkar SF, Bonetta D, McCourt P: **The ABSCISIC ACID INSENSITIVE 3 (ABI3) gene is modulated by farnesylation and is involved in auxin signaling and lateral root development in Arabidopsis**. *Plant J* 2003, **34**(1):67-75.

68. Tiwari SB, Wang XJ, Hagen G, Guilfoyle TJ: **AUX/IAA proteins are active repressors, and their stability and activity are modulated by auxin**. *Plant Cell* 2001, **13**(12):2809-2822.

69. Ulmasov T, Hagen G, Guilfoyle TJ: **ARF1, a transcription factor that binds to auxin response elements**. *Science* 1997, **276**(5320):1865-1868.

70. Grabherr MG, Haas BJ, Yassour M, Levin JZ, Thompson DA, Amit I, Adiconis X, Fan L, Raychowdhury R, Zeng Q *et al*: **Full-length transcriptome assembly from RNA-Seq data without a reference genome**. *Nat Biotechnol* 2011, **29**(7):644-652.

71. Anders S, Huber W: **Differential expression analysis for sequence count data**. *Genome Biol* 2010, **11**(10):R106.

72. Ernst J, Bar-Joseph Z: **STEM: a tool for the analysis of short time series gene expression data**. *BMC Bioinformatics* 2006, **7**:191.

73. Finn RD, Coggill P, Eberhardt RY, Eddy SR, Mistry J, Mitchell AL, Potter SC, Punta M, Qureshi M, Sangrador-Vegas A *et al*: **The Pfam protein families database: towards a more sustainable future**. *Nucleic Acids Res*

2016, **44**(D1):D279-285.

74. Tamura K, Dudley J, Nei M, Kumar S: **MEGA4: Molecular Evolutionary Genetics Analysis (MEGA) software version 4.0**. *Mol Biol Evol* 2007, **24**(8):1596-1599.
75. Guo AY, Zhu QH, Chen X, Luo JC: **[GSDS: a gene structure display server]**. *Yi Chuan* 2007, **29**(8):1023-1026.
76. Bailey TL, Boden M, Buske FA, Frith M, Grant CE, Clementi L, Ren J, Li WW, Noble WS: **MEME SUITE: tools for motif discovery and searching**. *Nucleic Acids Res* 2009, **37**(Web Server issue):W202-208.

Additional Files

Additional file 1: Table S1: Differentially expressed genes response to 1uM auxin in root libraries. The log2 (foldchange) value is positive and native mean that the gene is up-regulated and down-regulated, respectively.

Additional file 2: Table S2: Differentially expressed genes response to 50 uM auxin in root libraries. The log2 (foldchange) value is positive and native mean that the gene is up-regulated and down-regulated, respectively.

Additional file 3: Table S3 and Table S4: Pathways and proportions after KEGG analysis of differentially expressed genes in wheat roots. Table S3 and Table S4 correspond control *vs* 1uM auxin and control *vs* 50uM auxin, respectively.

Additional file 4: Figure S1: Profiles order based on the P-value significance of number assigned versus expected. The trend blocks with color ($p < 0.05$) showed a significant enrichment trend, and the trend blocks with similar trends had the same color. The trend block without color is the trend of non-significant enrichment.

Additional file 5: Table S5: List of the *TabZIP* sequences. Table S6: List of the *AtbZIP* sequences and *OsbZIP* sequences. Table S7: The structural features of motif 1-10. Table S8: Expression (FPKM) of *TabZIP* genes in response to different concentrations of auxin in wheat roots. Table S9: Sequences of primers used in qRT-PCR .

Tables

Table 1 Statistics of the read alignments in the RNA-Seq study

Sample name	Raw reads	Clean reads	clean bases	Clean reads Q20 (%)	Clean reads Q30 (%)	GC content of clean reads (%)	Total mapped rate (%)	Uniquely mapped (%)
CK_1	71,872,804	71,172,440	10.58G	96.81	91.83	53.11	88.82	82.55
CK_2	82,955,766	82,294,016	12.24G	97.15	92.54	53.51	88.31	81.46
CK_3	74,667,486	73,948,758	11.00G	96.88	91.99	53.68	88.81	82.12
1uM_1	72,090,192	71,550,684	10.65G	97.28	92.79	53.42	90.28	83.46
1uM_2	73,574,886	72,992,414	10.86G	97.2	92.62	53.71	90.14	83.50
1uM_3	73,122,628	72,270,476	10.74G	96.5	91.18	53.59	89.67	82.66
50uM_1	72,794,392	71,312,538	10.57G	95.91	89.28	53.61	90.80	83.90
50uM_2	84,039,152	82,720,674	12.27G	96.35	90.16	53.2	91.73	85.25
50uM_3	81,265,588	80,042,326	11.87G	96.36	90.13	53.49	92.36	85.19

The numbers 1–3 after CK, 1uM and 50uM identify the three independent biological replicates for the control and auxin treatments, respectively.

Q20: The percentage of bases with a Phred value > 20

Q30: The percentage of bases with a Phred value > 30

Table 2 20 top KEGG pathways with high representation of the DEGs

Pathway	DEGs genes with pathway annotation				ID
	All_profiles(629)	Profile0(159)	Profile1(298)	Profile6(65)	
Ribosome	47(7.47%)	15(9.43%)	17(5.70%)	0(0.00%)	ko03010
Starch and sucrose metabolism	45(7.15%)	16(10.06%)	17(5.70%)	5(7.69%)	ko00500
Plant hormone signal transduction	41(6.52%)	9(5.66%)	25(8.39%)	1(1.54%)	ko04075
Phenylpropanoid biosynthesis	36(5.72%)	8(5.03%)	16(5.37%)	7(10.77%)	ko00940
Photosynthesis	36(5.72%)	5(3.14%)	31(10.40%)	0(0.00%)	ko00195
Carbon metabolism	32(5.09%)	5(3.14%)	24(8.05%)	0(0.00%)	ko01200
Biosynthesis of amino acids	30(4.77%)	12(7.55%)	12(4.03%)	1(1.54%)	ko01230
Plant-pathogen interaction	26(4.13%)	3(1.89%)	5(1.68%)	12(18.46%)	ko04626
Pentose and glucuronate interconversions	24(3.82%)	8(5.03%)	12(4.03%)	2(3.08%)	ko00040
Amino sugar and nucleotide sugar metabolism	24(3.82%)	11(6.92%)	9(3.02%)	2(3.08%)	ko00520
Flavonoid biosynthesis	19(3.02%)	3(1.89%)	3(1.01%)	9(13.85%)	ko00941
Oxidative phosphorylation	18(2.86%)	1(0.63%)	7(2.35%)	1(1.54%)	ko00190
Glycolysis /Gluconeogenesis	18(2.86%)	1(0.63%)	16(5.37%)	0(0.00%)	ko00010
Carbon fixation in photosynthetic organisms	16(2.54%)	0(0.00%)	15(5.03%)	0(0.00%)	ko00710
Purine metabolism	16(2.54%)	3(1.89%)	10(3.36%)	2(3.08%)	ko00230
Pyrimidine metabolism	15(2.38%)	3(1.89%)	9(3.02%)	2(3.08%)	ko00240
Circadian rhythm - plant	15(2.38%)	1(0.63%)	5(1.68%)	7(10.77%)	ko04712
Photosynthesis - antenna proteins	14(2.23%)	1(0.63%)	13(4.36%)	0(0.00%)	ko00196
Glutathione metabolism	14(2.23%)	2(1.26%)	9(3.02%)	1(1.54%)	ko00480
Phosphatidylinositol	14(2.23%)	3(1.89%)	4(1.34%)	5(7.69%)	ko04070

signaling system					
Porphyrin and chlorophyll metabolism	14(2.23%)	3(1.89%)	11(3.69%)	0(0.00%)	ko00860

Table 3 Characteristics of *TabZIPs* responding to different concentrations of auxin.

ID	group	motif	intron
TabZIP6B_141	group4	4	3
TabZIP7A_158	group9	2,5,6,8,10	3
TabZIP6D_147	group4	4	3
TabZIP7D_169	group4	4	3
TabZIP5A_103	group6	2	7
TabZIP1D_15	group1	1	3
TabZIP2D_38	group5	2	1
TabZIP5D_130	group6	2	7
TabZIP5B_118	group7	2,9	6
TabZIP7A_149	group7	2,9	5
TabZIP5D_127	group8	2,9	0
TabZIPU_181	group8	2,9	0
TabZIP5B_109	group9	2,5,6,8,10	3
TabZIP6A_134	group9	2,5,6,8,10	4
TabZIP3A_46	group8	2,9	0
TabZIP6D_144	group9	2,5,6,8,10	4
TabZIP1A_5	group2	4,9	1
TabZIPU_182	group5	2	2
TabZIP7D_170	group7	2,9	5
TabZIP2D_37	group5	2	1
TabZIP7B_167	group8	2,9	0
TabZIP7B_161	group5	2	2

Figures

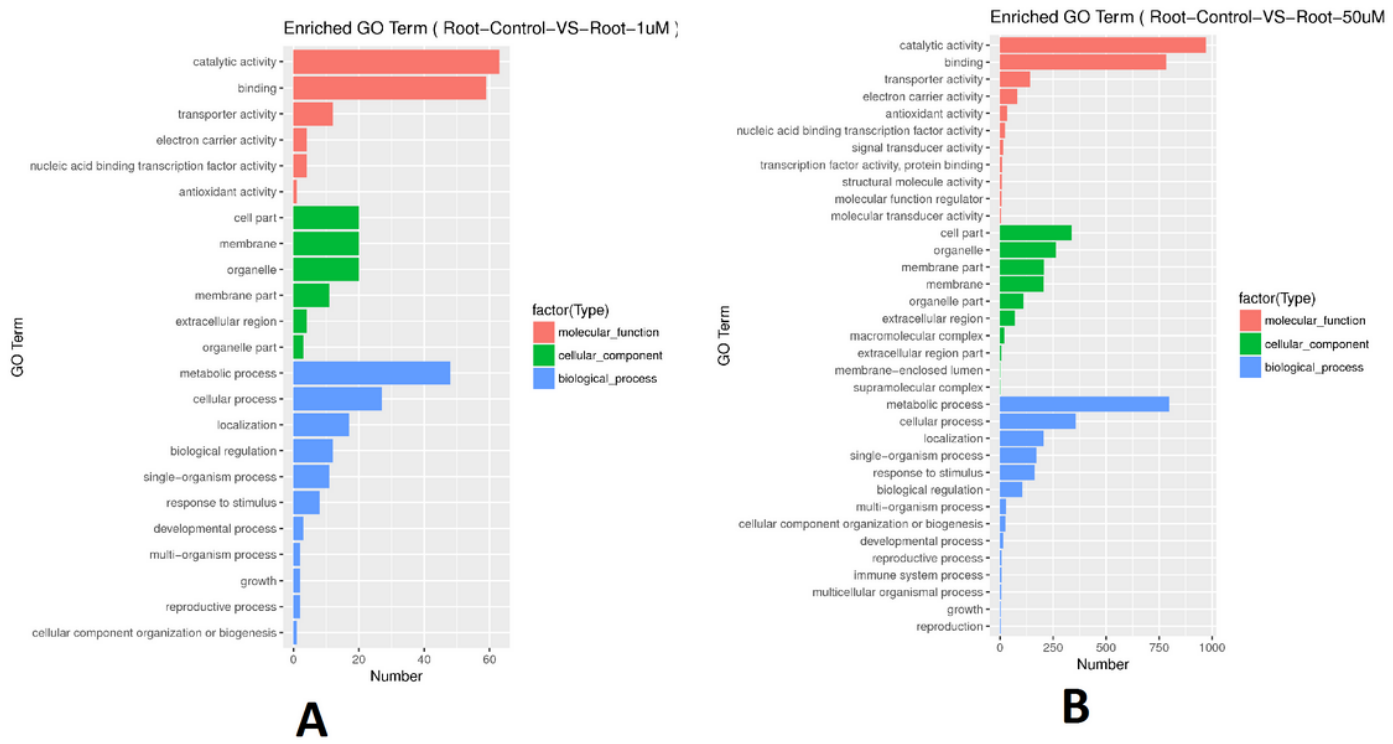

Figure 1

Histogram of Gene Ontology (GO) classification for wheat roots in defferent treatments. The results are summarized in three main categories: Molecular Function, Cellular Component and Biological Process terms. The x-axis represents the number of DEGs in each category and the y-axis indicates the subcategories. The subset “Root-control vs Root-1uM” (panel a) indicates the number of DEGs between control and 1uM auxin treatment, “Root-control vs Root-50uM” (panel b) indicates the number of DEGs between control and 50 uM auxin treatment.

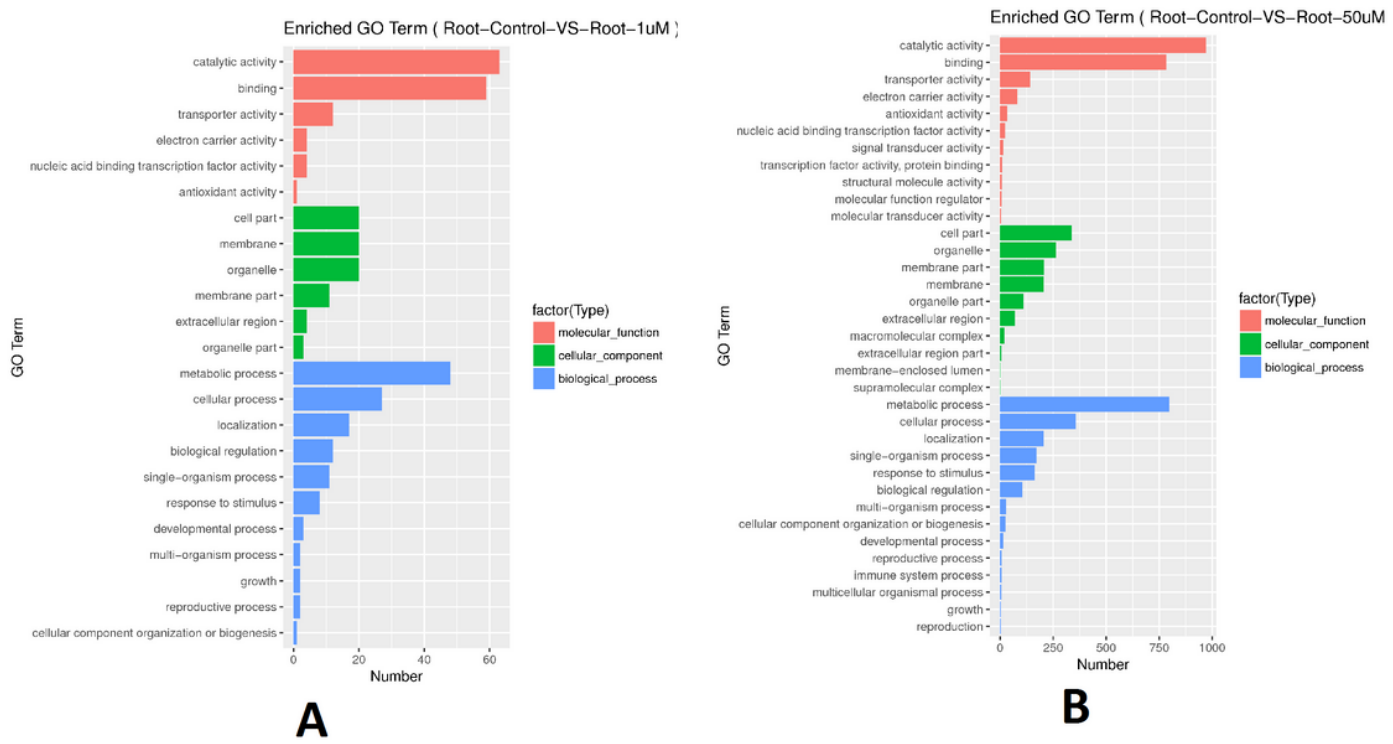

Figure 1

Histogram of Gene Ontology (GO) classification for wheat roots in defferent treatments. The results are summarized in three main categories: Molecular Function, Cellular Component and Biological Process terms. The x-axis represents the number of DEGs in each category and the y-axis indicates the subcategories. The subset “Root-control vs Root-1uM” (panel a) indicates the number of DEGs between control and 1uM auxin treatment, “Root-control vs Root-50uM” (panel b) indicates the number of DEGs between control and 50 uM auxin treatment.

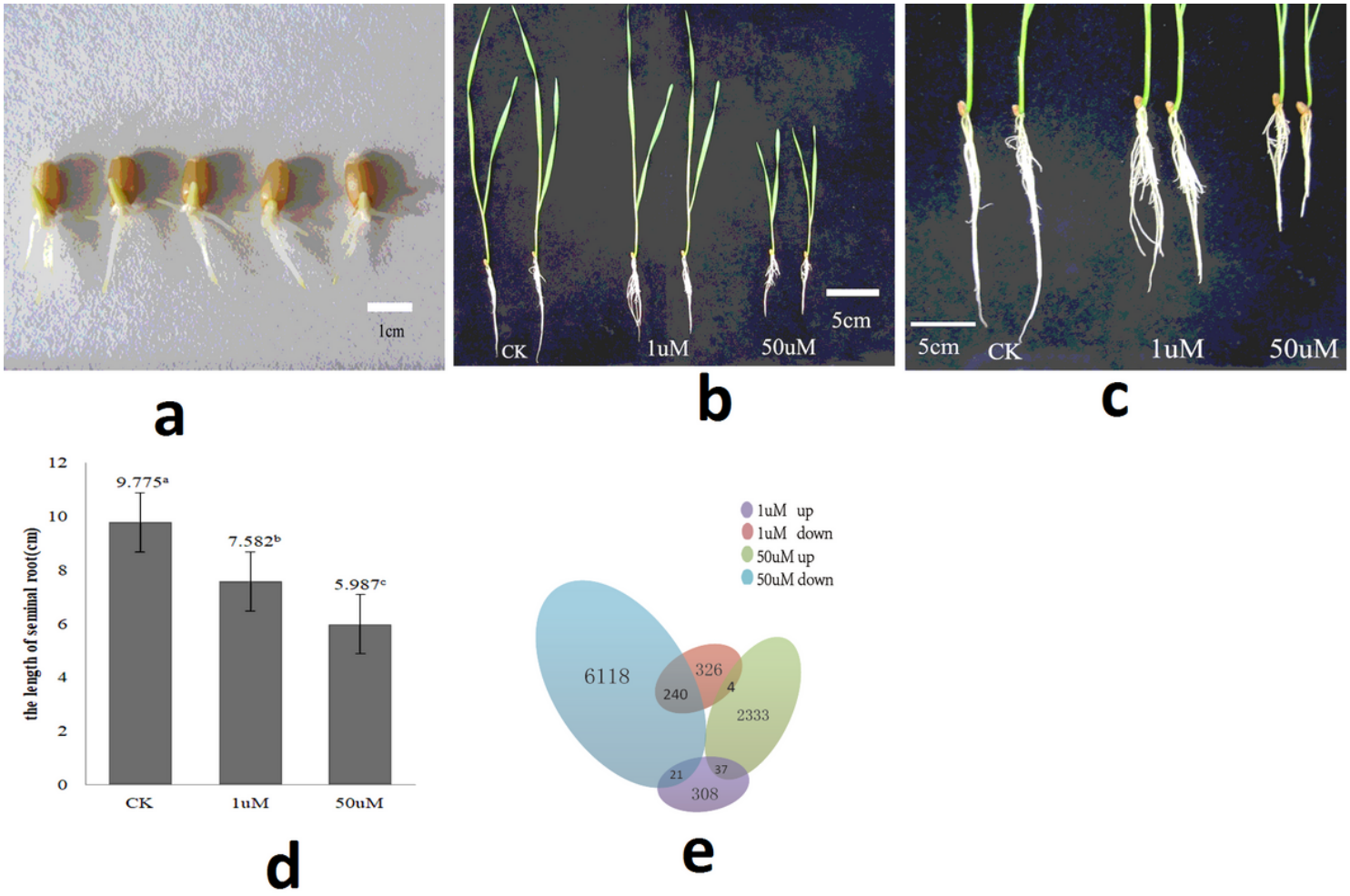

Figure 2

Phenotypic and gene expression responses of wheat roots in control and 1uM, 50uM auxin. a-c: The appearance of root under CK, 1uM and 50uM auxin at 14th day, the growth of roots was inhibited, and the growth of leaves was significantly inhibited by 50uM auxin. d: Significant comparison of seminal root length of at least 15 samples under each treatment. e: Differentially expressed genes (DEGs) under different treatments.

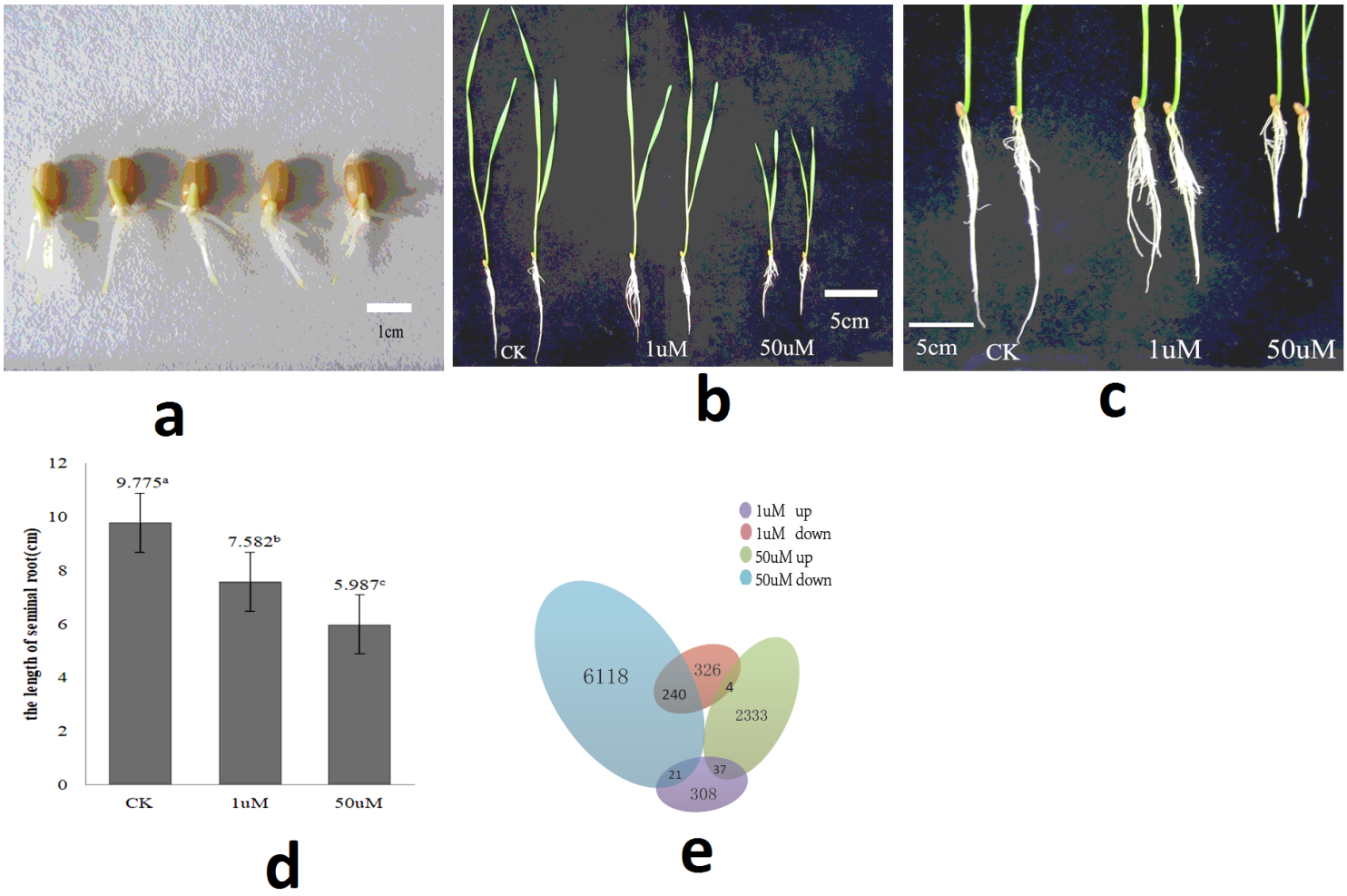

Figure 2

Phenotypic and gene expression responses of wheat roots in control and 1uM, 50uM auxin. a-c: The appearance of root under CK, 1uM and 50uM auxin at 14th day, the growth of roots was inhibited, and the growth of leaves was significantly inhibited by 50uM auxin. d: Significant comparison of seminal root length of at least 15 samples under each treatment. e: Differentially expressed genes (DEGs) under different treatments.

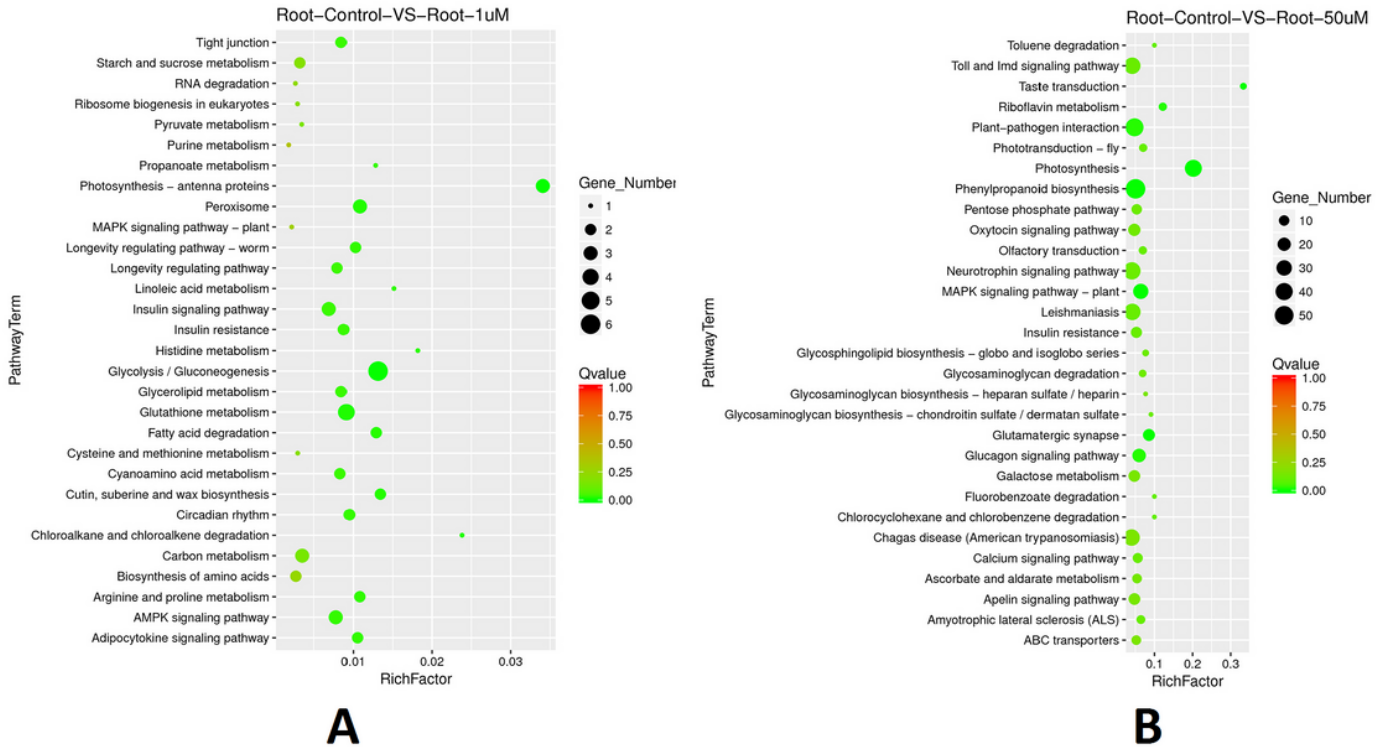

Figure 3

Scatter plot of KEGG pathway enrichment statistics for DEGs in wheat roots. Rich Factor is the ratio of differentially expressed gene numbers annotated in this pathway term to all gene numbers annotated in this pathway term. Greater Rich Factor means greater intensiveness. q-value is corrected p-value ranging from 0-1, and its less value means greater intensiveness. The subset “Root-control vs Root-1uM” (panel a) indicates the pathways enrichment under treatment of 1uM auxin. The subset “Root-control vs Root-1uM” (panel b) indicates the pathways enrichment under treatment of 50uM auxin.

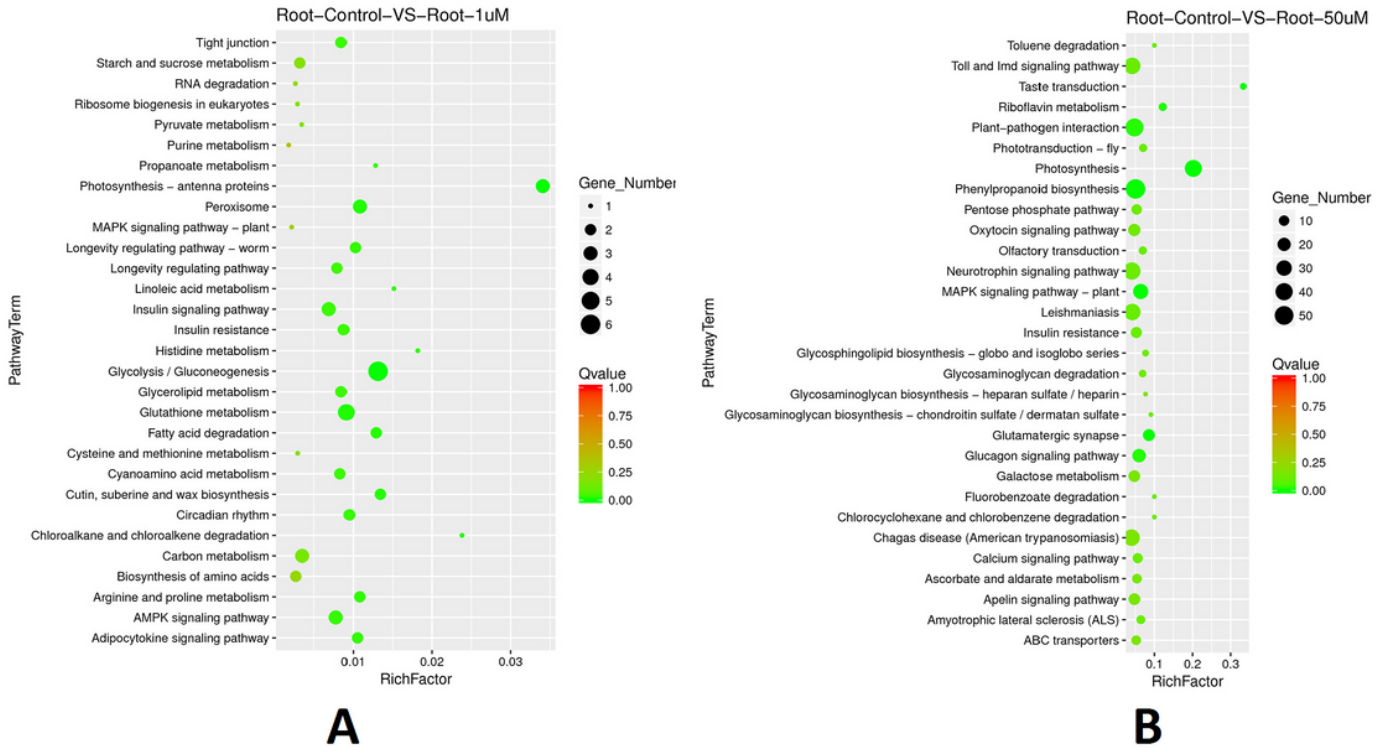

Figure 3

Scatter plot of KEGG pathway enrichment statistics for DEGs in wheat roots. Rich Factor is the ratio of differentially expressed gene numbers annotated in this pathway term to all gene numbers annotated in this pathway term. Greater Rich Factor means greater intensiveness. q-value is corrected p-value ranging from 0-1, and its less value means greater intensiveness. The subset “Root-control vs Root-1uM” (panel a) indicates the pathways enrichment under treatment of 1uM auxin. The subset “Root-control vs Root-1uM” (panel b) indicates the pathways enrichment under treatment of 50uM auxin.

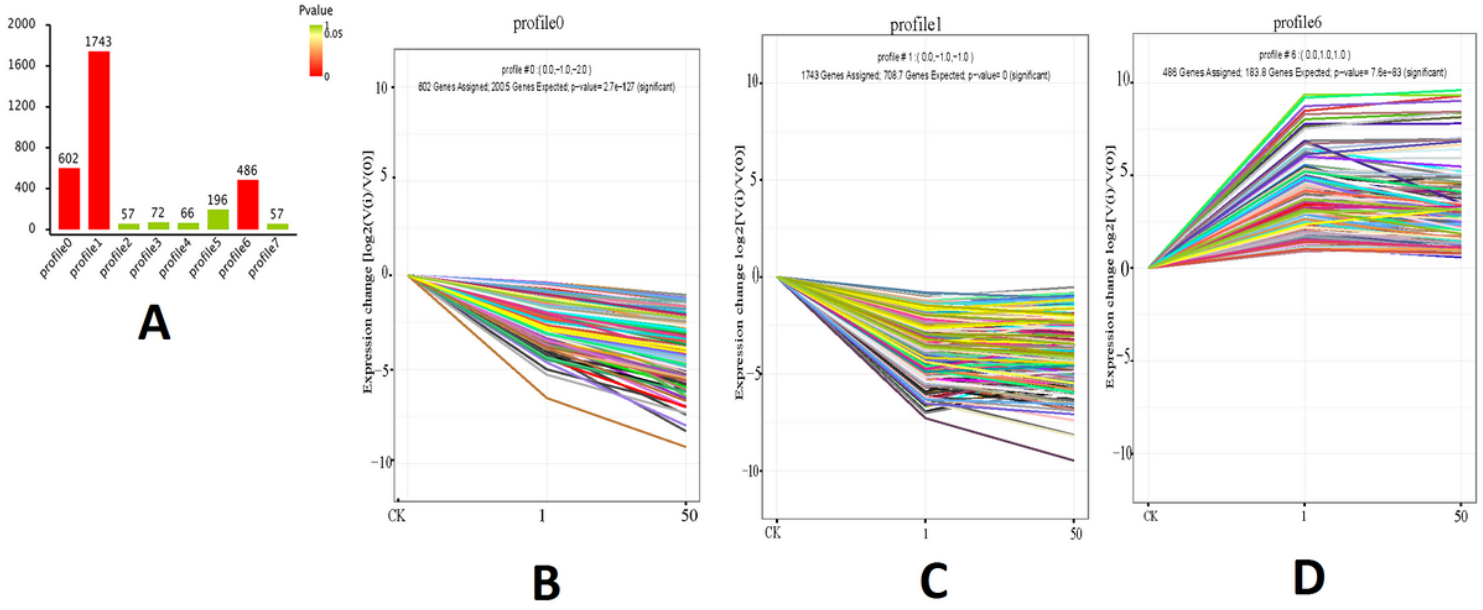

Figure 4

Three main DEGs expression profiles (p-value≤0.05) in eight profiles. a: Unigenes expression comparison between eight profiles. b-c: the two down-regulated patterns under auxin treatments. d: the up-regulated patterns under auxin treatments.

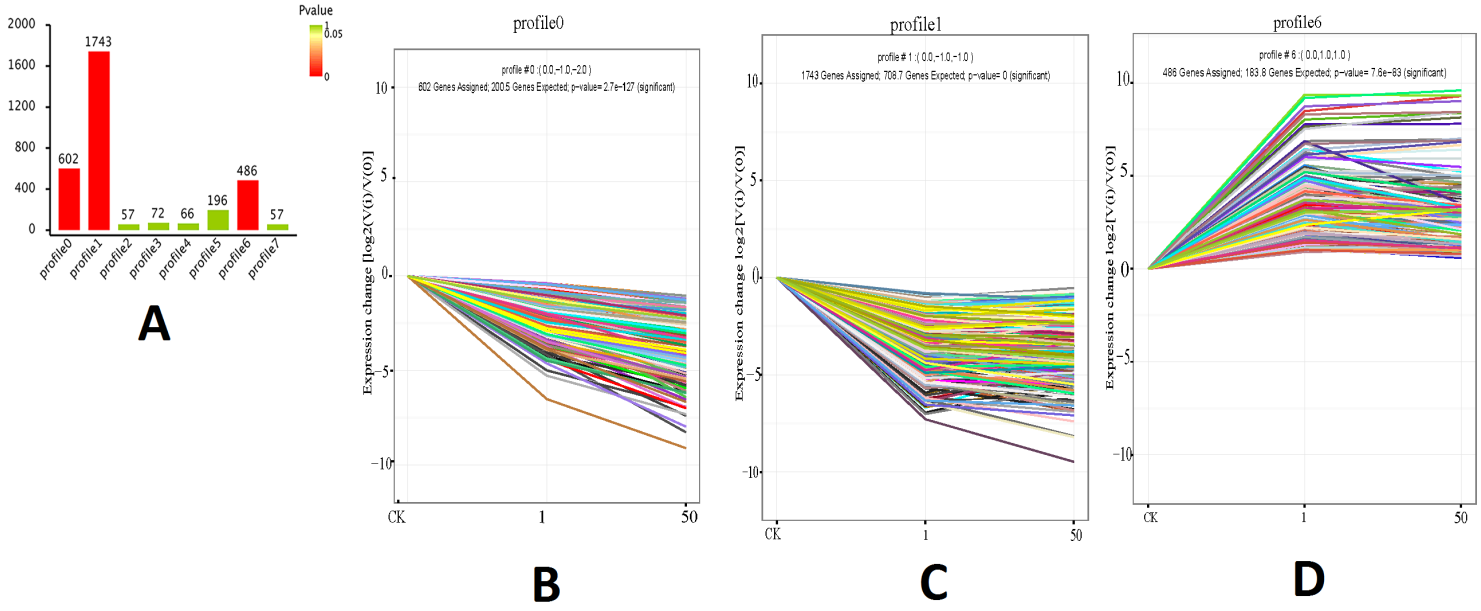

Figure 4

Three main DEGs expression profiles (p-value≤0.05) in eight profiles. a: Unigenes expression comparison between eight profiles. b-c: the two down-regulated patterns under auxin treatments. d: the up-regulated patterns under auxin treatments.

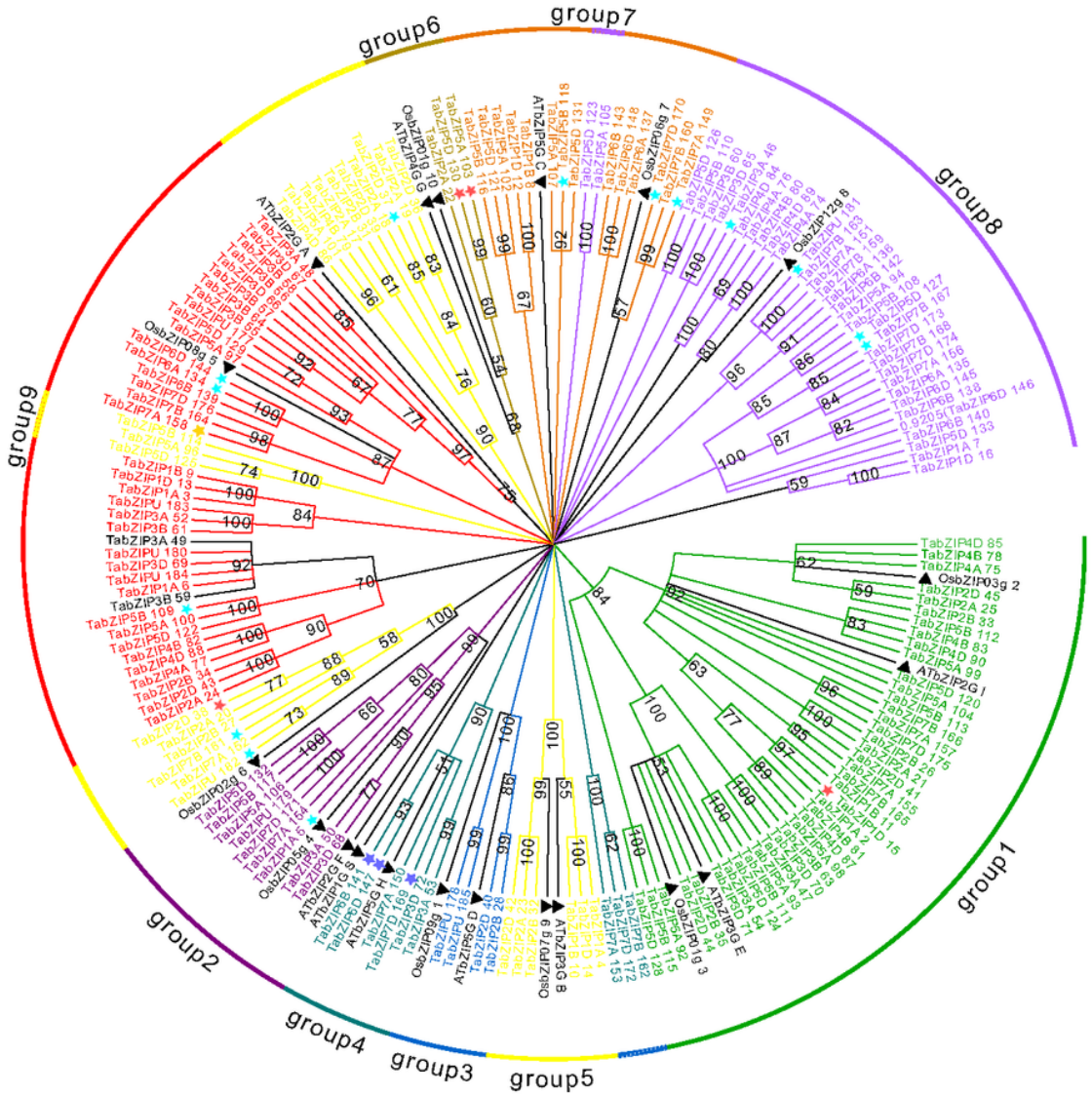

Figure 5

Unrooted phylogenetic tree representing relationships among bZIP domains of wheat, rice and Arabidopsis. The different-colored arcs indicate different groups (or subgroups) of bZIP genes. The black solid triangle represent bZIP genes with the prefix ‘Os’ and ‘At’ from rice and Arabidopsis respectively. The colored stars represent TabZIP genes differentially expressed under different concentrations of auxin treatment. The evolutionary history was inferred using the Neighbor-Joining method. The bootstrap consensus tree inferred from 1000 replicates is taken to represent the evolutionary history of the taxa analyzed. Branches

corresponding to partitions reproduced in less than 50% bootstrap replicates are collapsed. The evolutionary distances were computed using the Poisson correction method and are in the units of the number of amino acid substitutions per site. The analysis involved 196 amino acid sequences. All positions containing gaps and missing data were eliminated. Evolutionary analyses were conducted in MEGA7.

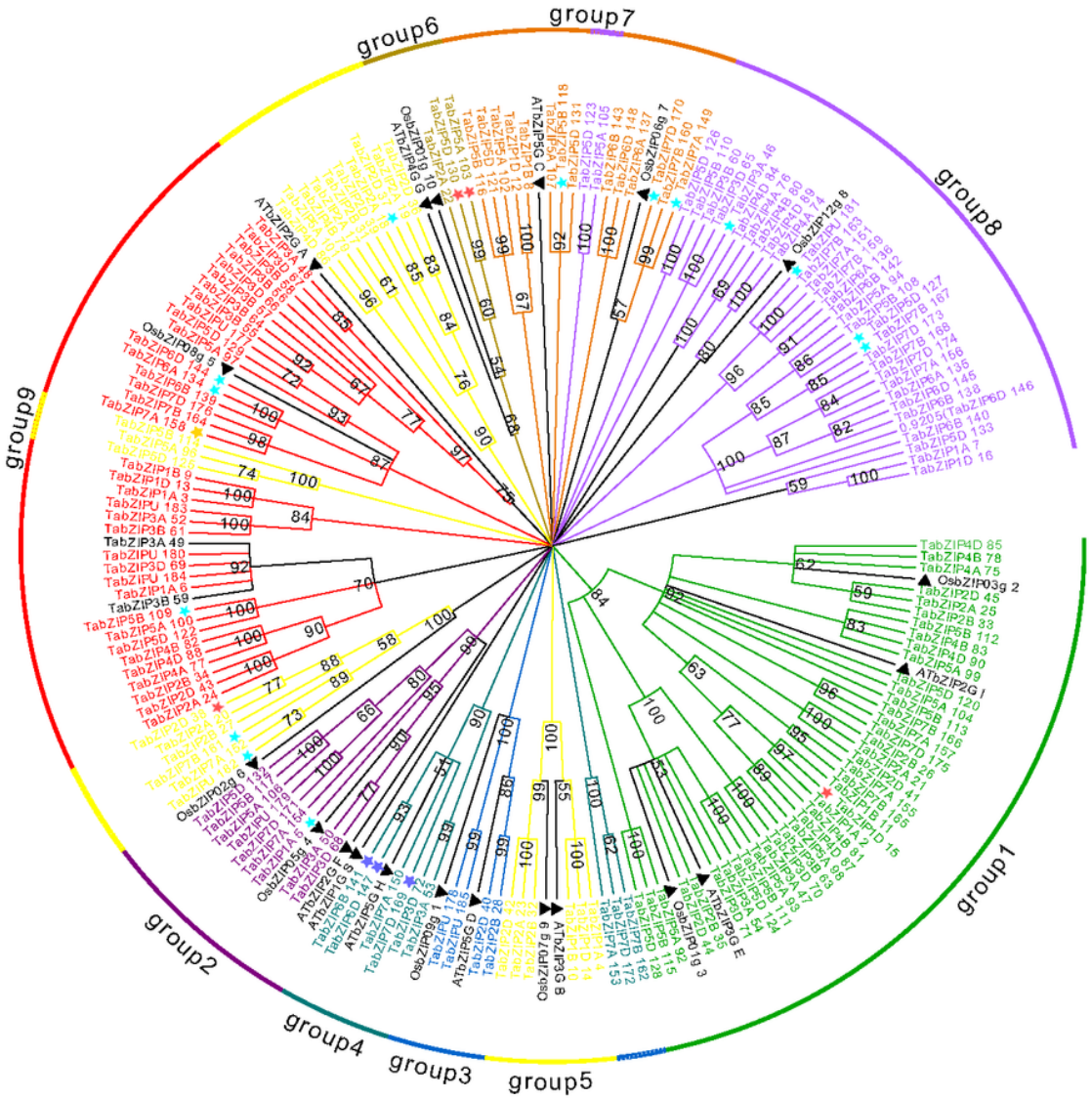

Figure 5

Unrooted phylogenetic tree representing relationships among bZIP domains of wheat, rice and Arabidopsis. The different-colored arcs indicate different groups (or subgroups) of bZIP genes. The black solid triangle

represent bZIP genes with the prefix ‘Os’ and ‘At’ from rice and Arabidopsis respectively. The colored stars represent TabZIP genes differentially expressed under different concentrations of auxin treatment. The evolutionary history was inferred using the Neighbor-Joining method. The bootstrap consensus tree inferred from 1000 replicates is taken to represent the evolutionary history of the taxa analyzed. Branches corresponding to partitions reproduced in less than 50% bootstrap replicates are collapsed. The evolutionary distances were computed using the Poisson correction method and are in the units of the number of amino acid substitutions per site. The analysis involved 196 amino acid sequences. All positions containing gaps and missing data were eliminated. Evolutionary analyses were conducted in MEGA7.

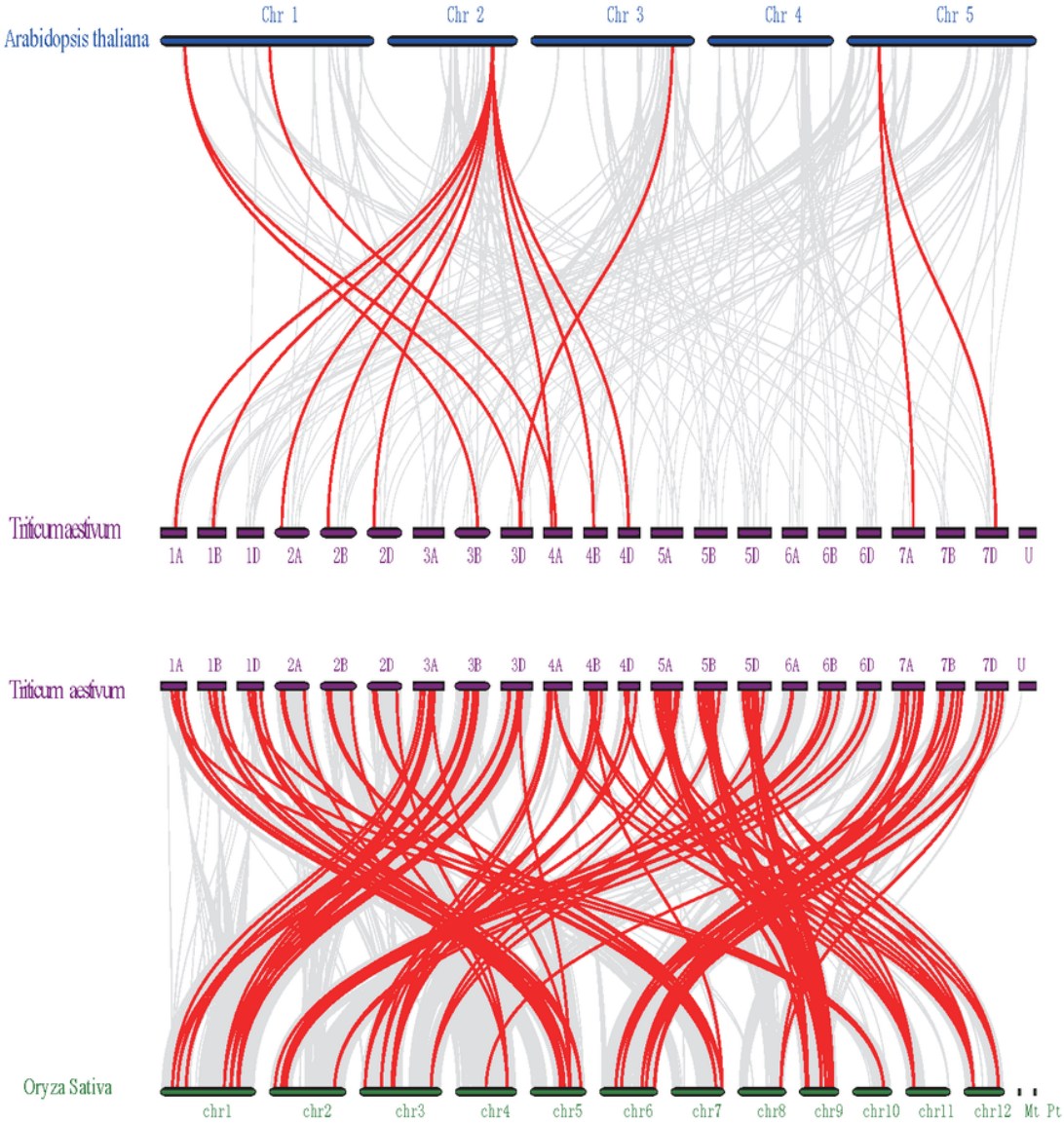

Figure 6

Comparative syntenic maps of bZIP genes between wheat and two representative plant species. Gray lines in the background indicate the collinear blocks within wheat and other plant genomes, while the red lines highlight the syntenic bZIP gene pairs.

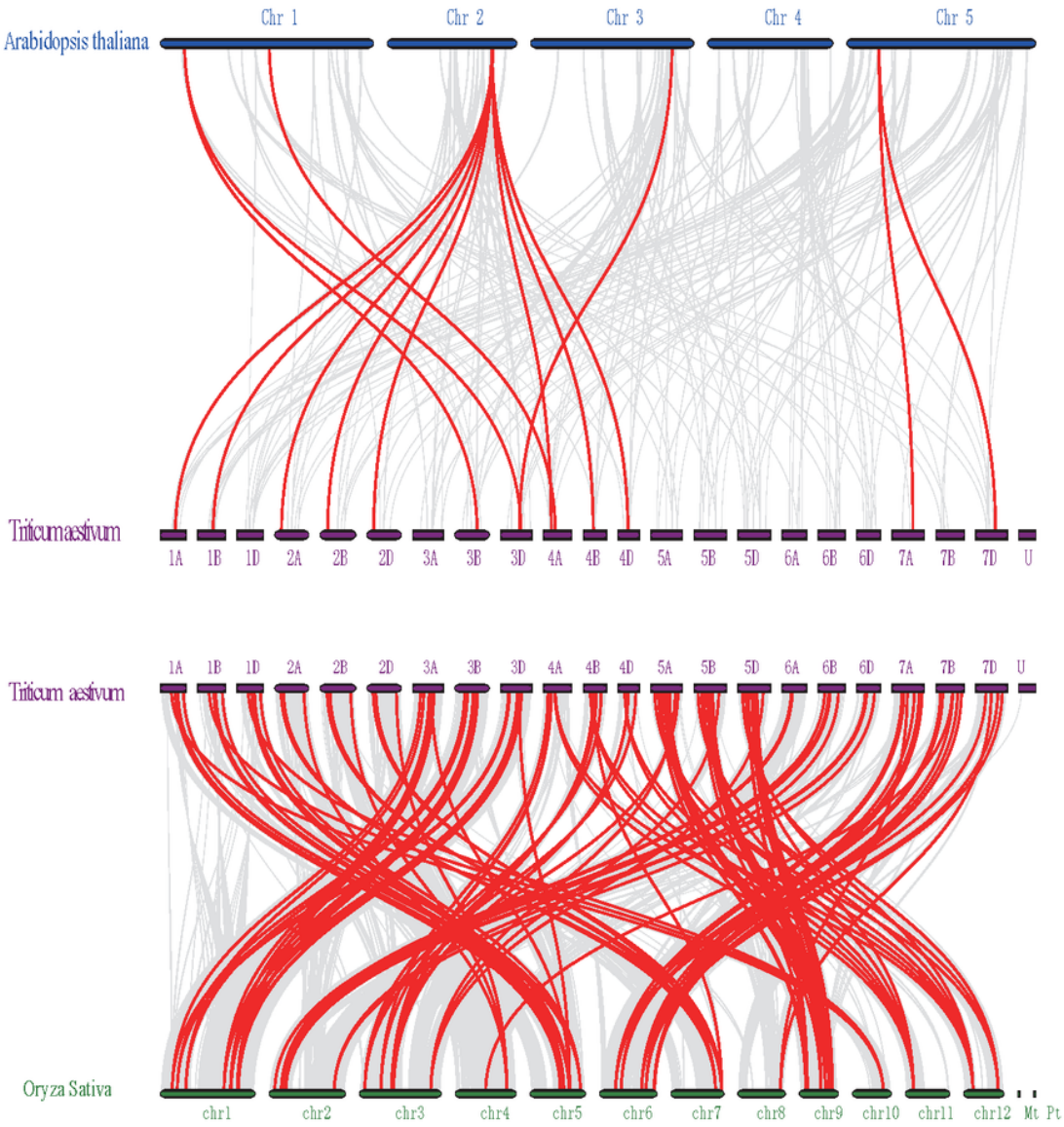

Figure 6

Comparative syntenic maps of bZIP genes between wheat and two representative plant species. Gray lines in the background indicate the collinear blocks within wheat and other plant genomes, while the red lines

highlight the syntenic bZIP gene pairs.

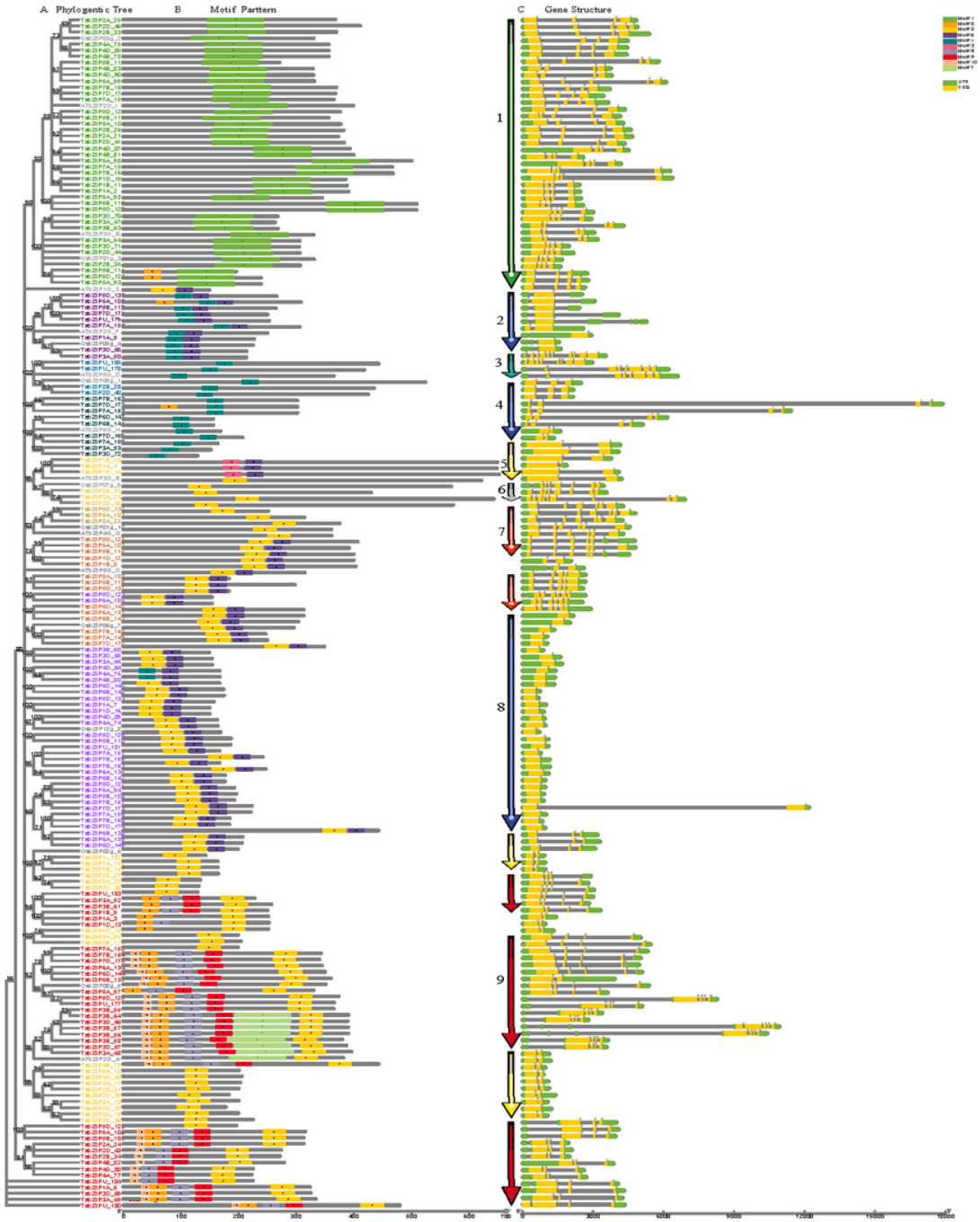

Figure 7

Phylogenetic relationships, gene structure and architecture of conserved protein motifs in TabZIP genes. a: The phylogenetic tree was constructed based on the full-length sequences of TabZIP proteins using MEGA 7 software. Details of clusters are shown in different colors. b: The motif composition of TabZIP proteins. The motifs, numbers 1–10, are displayed in different colored boxes. c: Exon-intron structure of TabZIP genes. Green boxes indicate untranslated 5'-and 3'-regions; yellow boxes indicate exons; black lines indicate introns.

The number indicates the phases of corresponding introns. The length of protein can be estimated using the scale at the bottom.

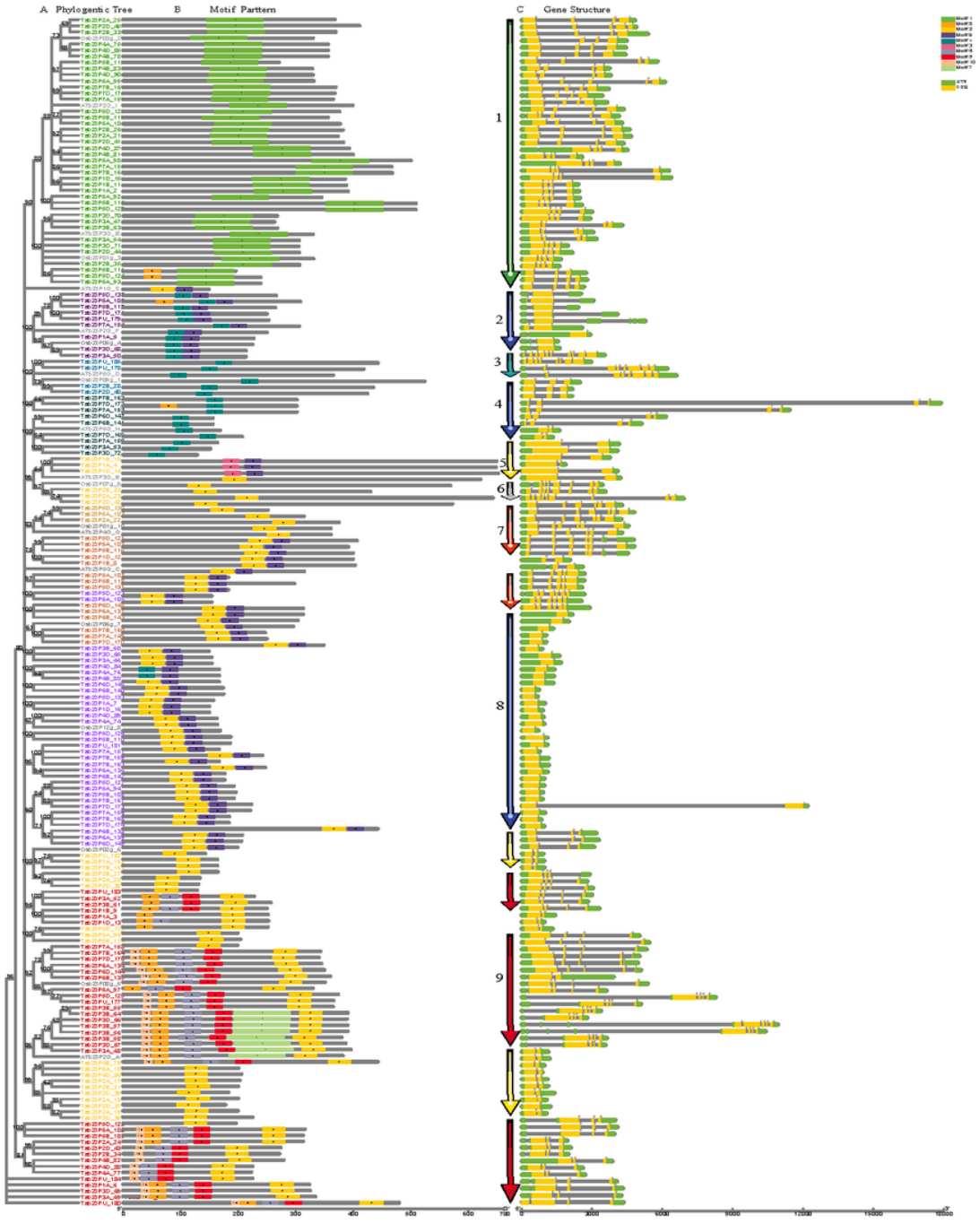

Figure 7

Phylogenetic relationships, gene structure and architecture of conserved protein motifs in TabZIP genes. a: The phylogenetic tree was constructed based on the full-length sequences of TabZIP proteins using MEGA 7 software. Details of clusters are shown in different colors. b: The motif composition of TabZIP proteins. The motifs, numbers 1–10, are displayed in different colored boxes. c: Exon-intron structure of TabZIP genes.

Green boxes indicate untranslated 5'-and 3'-regions; yellow boxes indicate exons; black lines indicate introns. The number indicates the phases of corresponding introns. The length of protein can be estimated using the scale at the bottom.

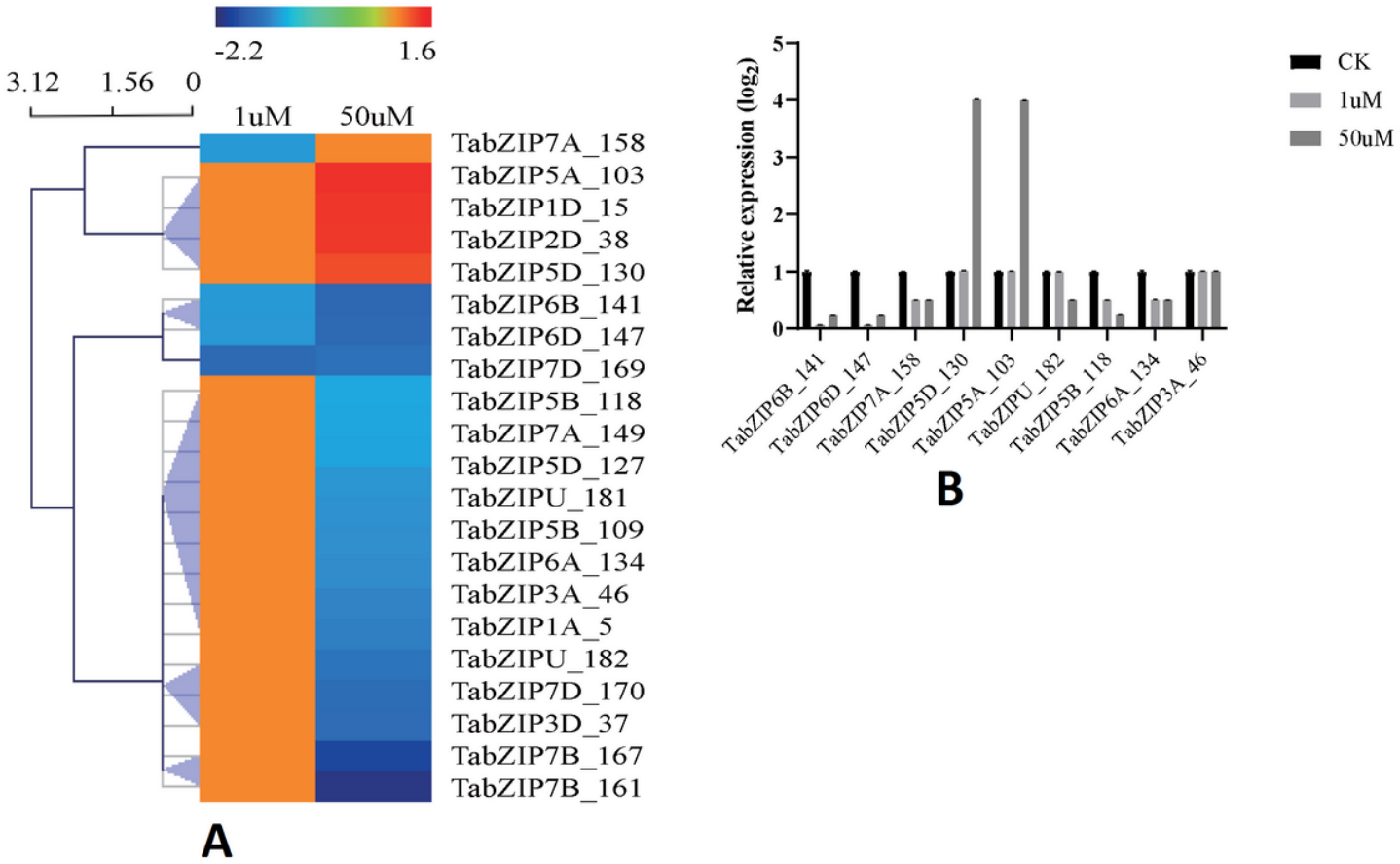

Figure 8

The Expression of TabZIP genes under different auxin concentrations. a: RNA-seq data were used to produce the heat maps. b: qPCR validation for 9 DEGs identified by RNA-Seq in the comparison between CK, 1uM and 50uM auxin treatments.

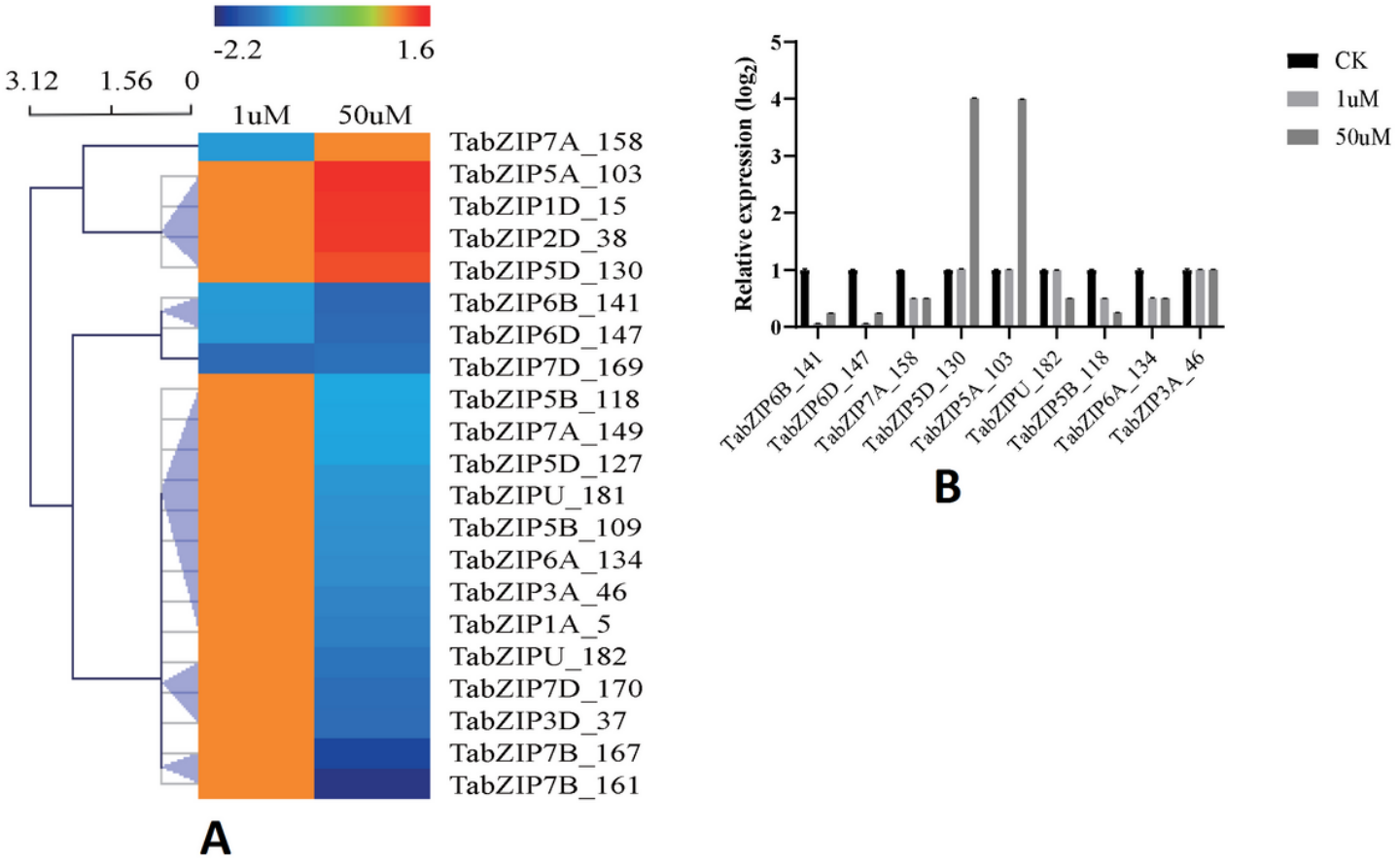

Figure 8

The Expression of TabZIP genes under different auxin concentrations. a: RNA-seq data were used to produce the heat maps. b: qPCR validation for 9 DEGs identified by RNA-Seq in the comparison between CK, 1uM and 50uM auxin treatments.

Supplementary Files

This is a list of supplementary files associated with this preprint. Click to download.

- Additionalfile1.xlsx
- Additionalfile1.xlsx
- Additionalfile2.xlsx
- Additionalfile2.xlsx
- Additionalfile3.xlsx
- Additionalfile3.xlsx
- Additionalfile4.docx
- Additionalfile4.docx
- Additionalfile5.xlsx

- Additionalfile5.xlsx